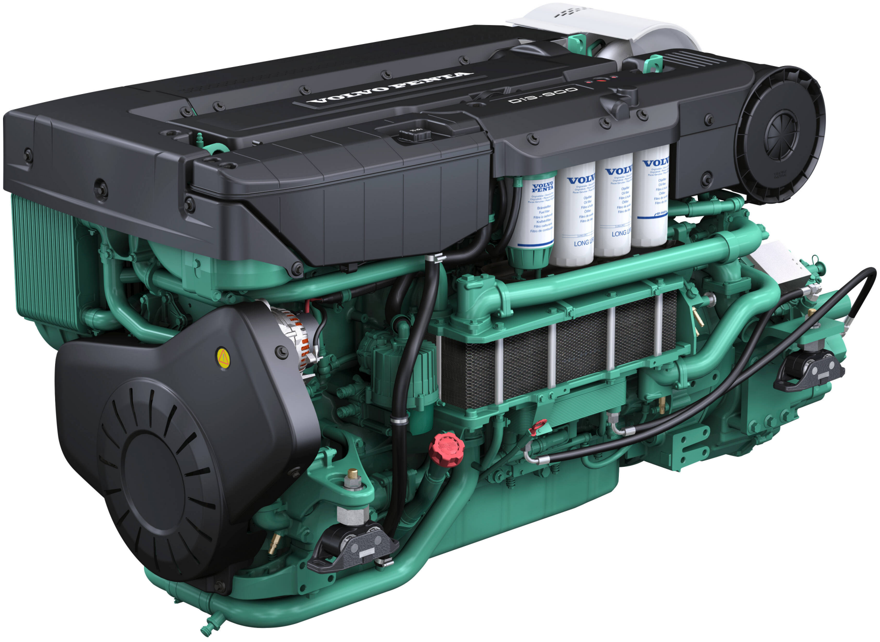

1D Model Development And Simulation of Low-Grade Waste Heat Recovery From a Marine Engine

Potential of low grade heat recovery in the Volvo D13 Engine for Marine application

Master's thesis in Sustainable Energy Systems

VARUN BHANDARI

DEPARTMENT OF SPACE EARTH AND ENVIRONMENT

Chalmers University of Technology
Gothenburg, Sweden 2021
www.chalmers.se

Master thesis project Report

1D model development and simulation of low-grade waste heat recovery from a marine engine

Varun Bhandari
Chalmers University of Technology
Department of Space, Earth and Environment
bhandari@student.chalmers.se

June 15, 2021

Low Grade Waste Heat Recovery in a Marine Diesel Engine
Development of Computational model in SIMULINK
Varun Bhandari

Supervisor: Francesco Galuppo, Volvo Penta
Examiner: Stavros Papadokonstantakis, Department of Space Earth and Environment

Master's Thesis 2021
Department of Space, Earth and Environment
Division of Energy Technology
Chalmers University of Technology
SE-412 96 Gothenburg
Telephone +46 31 772 1000

Cover: Volvo Marine D13 engine.

Typeset in LaTeX
Printed by Chalmers Reproservice
Gothenburg, Sweden 2021

Abstract

The increasing awareness about the effect of emission of CO_2 into the atmosphere, as well as meeting the emission targets set by IMO (International Marine Organization) by 2050 results in a continuous need for improving efficiencies of marine engines. A large portion of the fuel's chemical energy is lost to the surroundings as heat, even in the most energy efficient engines. Waste heat recovery through a rankine cycle has emerged as a promising way to increasing the engine efficiency by utilizing the untapped availability of waste heat in the coolant systems as well as the exhaust of the engine.

The highly transient nature of operation of an engine and depicting the heat transfer phenomenon in an ORC (Organic Rankine Cycle) accurately makes the representation of an ORC through a mathematical model quite challenging. Based on the application, selection of the right working fluid, equipment and control strategy is crucial for the performance of the ORC

In this thesis, a Simulink based mathematical model of an ORC for waste heat recovery from a marine engine is built. The WHR (Waste Heat Recovery) model is built for transient operation. The model is run on a road cycle, built from actual field test data of a boat, to simulate its performance in actual operation of the marine vessel. Further, the performance of ORC with different working fluids and different type of expanders is evaluated. And finally, a rough cost estimation of the ORC is done.

The results from the project show that the refrigerant R1234ze(Z) is the most suitable for engine coolant WHR application and turbine expander performs better than the volumetric expander. Lastly, as the scale of the ORC system increases, it becomes increasingly cost effective.

Acknowledgement

The thesis work was carried out in the Computer Aided Engineering department at Volvo Penta, Gothenburg from January 2021 to June 2021. I would like to take this opportunity to thank everyone who has helped me to complete the thesis successfully.

I would like to thank Francesco Galuppo, my supervisor at Volvo Penta for all the guidance and support during the thesis. I would also like to thank my examiner Stavros Papadokonstantakis, from the Department of Space, Earth and Environment (SEE) at Chalmers for his constant support and valuable feedback in this project. I would also like to express our gratitude to Peter Olsson from the CAE group for helping me during the project.

Contents

List of Figures

List of Tables

Nomenclature

η_P Pump Efficiency

η_T Turbine Efficiency

μ Fluid viscosity

ρ Fluid density

τ Time Constant

C_p Specific heat of fluid

CAC Charge Air Cooler

CFC Chlorofluorocarbon

COR Compression Ratio of Piston Expander

EOC Engine Oil Cooler

GOC Gearbox Oil Cooler

GWP Global Warming Potential

K_{wall} heat exchanger wall thermal conductivity

l Characteristic length of heat exchanger channel

$LMTD$ Log Mean Temperature Difference

m mass flow (kg/s)

N_{exp} Expander Speed

n_{exp} Number of expander cylinders

ODP Ozone Depletion Potential

ORC Organic Rankine Cycle

P_{act} Actual Pressure of working fluid

$P_{critical}$ Critical pressure of working fluid

$P_{critical}$ Critical Pressure of fluid

P_{red} Reduced pressure ratio of working fluid

P_{red} Reduced Pressure Ratio of fluid

q Fluid quality

t_{wall} heat exchanger wall thickness

V_{exp} Single Expander Cylinder Volume

wf working fluid

WHR Waste heat recovery

GHG Green House Gas

IEA International Energy Agency

kW Kilo Watts

Wh Watts Hours

1 Introduction

1.1 Purpose

Maritime transport is the backbone of international trade and the global economy. Around 80% of global trade by volume is carried by sea and the IEA (International Energy Agency) predicts a doubling of shipping tonne-kilometers(TKMS) between 2006 and 2050. [12] In 2015, 75 trillion TKMS were attributed to shipping. In recent years public concerns regarding the environmental impacts of maritime transport have increased. This is because maritime transport is the fifth largest contributor to air pollution and carbon emissions, and the growth rate of the emissions makes the problem even more pressing. Maritime transport is responsible for about 2.5% of global greenhouse gas (GHG) emissions and these emissions could grow between 50% to 250% by 2050.[10].

IMO (International Maritime Organization) is a specialized agency of the United Nations with mission: safe, clean and sustainable shipping.Its goal is the Reduction of CO_2 emissions for international shipping, by at least 40% by 2030, pursuing efforts towards 70% by 2050, compared to 2008 maritime emissions. These goals can only be satisfied by taking innovative measures in operation and technical design.

Marine industry is dominated by Internal Combustion Engines (ICE) which is a major source of pollution because of the CO_2 emission and other harmful emissions. Considering the total chemical energy of the fuel, roughly about 40-50% of the energy is available as useful shaft power. Rest of the energy is wasted in the form of heat, as seen in Figure 1. Reclaiming this waste heat for producing energy can lead to overall engine efficiency improvement and reduction of break specific fuel consumption of the engine (BSFC).

The concept of waste heat recovery and its utilization in another energy form is not a novel and futuristic concept.In the automotive field, turbocharging is used to improve overall energy efficiency of the engine using the waste heat from exhaust air. Driven by future pollution norms and fluctuating fuel prices, engine waste heat recovery is becoming more and more important.

Organic Rankine cycle (ORC) is one of the crucial technologies to recover the wasted heat in low to medium heat sources due to the simplicity, availability of the components and reliability. [6] The waste heat is converted to electricity using an ORC which can be used for various applications on the vehicle. The working fluid inside the ORC is boiled with the help of the heat source and is passed through an expander to produce usable work in terms of electric energy .Vaja and Gambarotta demonstrated in their study a 12 % increase in the overall engine efficiency when coupled with a bottoming ORC system.[14] Aly estimated that the heat recovered from diesel engine exhaust gases can be used to obtain an additional 15% to 16% increase in the total power output.[2] . As per Dolz, for a two stage turbocharged, 12 litre heavy duty diesel engine, the waste heat recovery efficiency can be as high as 6% when using a bottoming ORC system. [4].

The selection of working fluid for the waste heat recovery system is very important as the thermo-physical properties of a fluid determine its ideal pressure and temperature range for operation. A detailed study on the desirable properties of refrigerants for a low grade ORC has been carried out by Nouman [8]. Selecting the working fluid with the right boiling point, heat of vaporization, viscosity etc. is very important. The fluid should also have low GWP and should be safe during operation.

In the study by Tchanche, a few challenges of introducing an ORC system in an automobile engine have been discussed, [13]. Increase in investment & maintenance cost, increase in system complexity, low efficiency of small capacity expansion machines and life cycle environmental impact of working fluid and equipment are mentioned as the key challenges of an ORC system.

Chapter one of the thesis provides the motivation behind this study, scope of the project and delimitations. Chapter two provides the principles governing the Simulink and Aspen models, properties of working fluids and theory of controls. Chapter three explains the procedure followed for collection of data and building the Simulink and Aspen models. Chapter four describes the results from the Simulink and Aspen models. In Chapter five, a reflection of the work and the most important take away points are discusses along with future work.

1.2 Objective

The goal of this thesis is to investigate a Rankine based low-grade waste heat recovery system for marine application. The purpose of the ORC is to produce electricity from the excess heat in the engine. The ORC is built on thermodynamic and mathematical models which is implemented using Simulink software. Simulink also allows the easy representation of complex systems in terms of components and connections. Simulations are carried out for steady state as well as transient state. Performance of different working fluids for the Rankine cycle as well as different types of components are compared. Steady state models of ORC are also built using Aspen plus software and a techno-economic analysis is carried out from the software to get the cost estimate of the ORC system. The models are also tested on a road cycle of

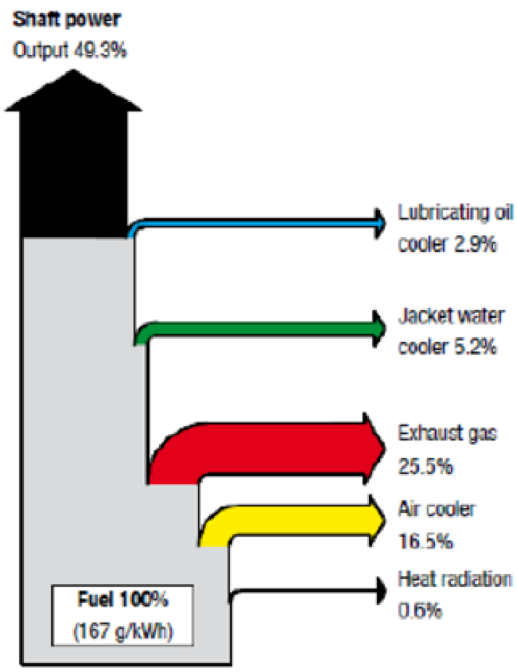

Figure 1: Fuel energy utilization of a diesel engine[9]

approx. two hours, built from real field test data collected for a boat
The thesis project is carried out at Volvo Penta, Gothenburg. The reference models and engine test data which is used in this thesis are provided by the company.

1.3 Delimitation

The quality of the results obtained from the model is dependent on the availability of the required data. When the necessary data is not available, approximations and assumptions are made for the models, which are listed in the report, and could lead to inaccuracies.
From the perspective of fluid selection, only the fluids which are readily available in the market are considered and not the ones which are under development. Even though, the next generation fluids might possess better performance than the current ones, they are not considered as sufficient data is not available.
The model is tested using actual engine test data which closely depict the actual operation of the ORC system in a marine engine. Experimental test validation of the ORC is not carried out in this thesis.

2 Theory

In this section, the working principles behind the ORC system will be presented along with the state of the art in this field of study.

2.1 Organic Rankine Cycle

A Rankine cycle is a thermodynamic cycle in which power is produced while interacting between a hot and a cold source. Water is the working fluid in a regular rankine system and it has four components- boiler, expander, condenser and a pump. An ideal Rankine cycle is represented in Figure 2. For extraction from a low temperature heat source, an ORC is used. An ORC is different from a regular Rankine cycles as it uses organic working fluids with low boiling points instead of water.The four key processes in the rankine cycle are

Process 1-2-Isentropic compression The working fluid is pumped from low to high pressure. The state of the working fluid is liquid. A small power is required for pumping the working fluid which can be expressed as Equation 1

$$\dot{W}_{pump} = \dot{m}_{wf} \frac{P_{pump,out} - P_{pump,in}}{\rho_{pump,in}} \tag{1}$$

Process 2-3-Isobaric heat addition The high pressure fluid enters the boiler where heat is added to the working fluid at constant pressure from the heat source. The working fluid changes phase in the evaporator to become saturated or super heated vapour.The heat addition in evaporator can be calculated as Equation 2

$$Q_{evap} = \dot{m}_{wf}(h_{evap,out} - h_{evap,in}) \tag{2}$$

Process 3-4-Isentropic expansion The vapour from the boiler is passed through the expander, where it generates power. In expanding, the vapour goes from high pressure to low pressure. Power generated by expander can be expressed as Equation 3

$$\dot{W}_{exp} = \dot{m}_{wf}(h_{exp,in} - h_{exp,out}) \tag{3}$$

Process 4-1- Isobaric heat rejection The working fluid at low pressure enters the condenser where it rejects heat to cold source to turn to liquid state. Heat rejected from condenser can be expressed as Equation 4

$$Q_{cond} = \dot{m}_{wf}(h_{cond,in} - h_{cond,out}) \tag{4}$$

The efficiency of the ORC system is given by Equation 5

$$\eta_{ORC} = \frac{\dot{W}_{exp} - \dot{W}_{pump}}{Q_{evap}} = \frac{(h_{wf,exp,in} - h_{wf,exp,out}) - (h_{wf,pump,out} - h_{wf,pump,in})}{h_{wf,evap,out} - h_{wf,evap,in}} \tag{5}$$

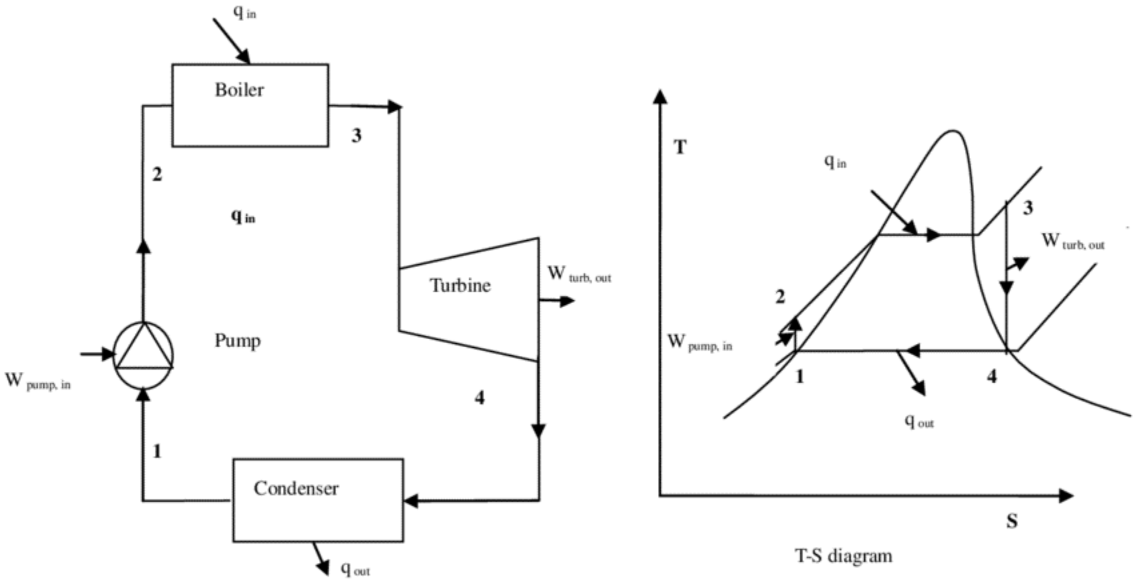

Figure 2: Ideal Rankine Cycle

The state of the fluid at the 4 different points are mentioned in the Table 4.

State point	Working fluid Temperature	Working fluid Pressure	Working fluid State
1	Low	Low	Liquid
2	Low	High	Liquid
3	High	High	Vapour
4	High	Low	Vapour

Table 1: State of working fluid at different points in an ORC

In reality, the expansion and compression process is not isentropic. Due to irreversibilities in the system the net power output of the actual cycle is always less than the ideal cycle. The pump and expander efficiencies account for the irreversibilities in the equipment, and are given by Equation 6 and 7. The "′" represents ideal process.

$$\eta_{pump} = \frac{ideal\ work}{actual\ work} = \frac{h'_{wf,pump,out} - h_{wf,pump,in}}{h_{wf,pump,out} - h_{wf,pump,in}} \tag{6}$$

$$\eta_{exp} = \frac{actual\ work}{ideal\ work} = \frac{h_{wf,exp,in} - h_{wf,exp,out}}{h_{wf,exp,in} - h'_{wf,exp,out}} \tag{7}$$

2.2 Components of ORC

2.2.1 Expander

The expander is the machine that extracts the energy from the expansion of high-pressure vapour and converts fluid energy to mechanical energy. Expander is the most crucial part of the ORC system as well as the most costly.[1] The choice of the expander depends on a number of factors such as the working fluid used, operating pressure-temperature range, size & weight restrictions, speed range etc. Expanders are of two types, namely turbo machine type expanders (velocity type) such as radial, axial turbines and displacement type expanders (volumetric type) such as piston cylinder, screw, rotary vane type.

Volumetric Expander

The piston cylinder expander, or reciprocating expander is one of the expander types used in this model since the application required low working fluid flow rate. The low rotational speed of the expander allows it to directly attach to the generator without the need for a gearbox.[1]

Figure 3 represents the expansion process of the working fluid by a Pressure Volume diagram. Table 2 provides a brief explanation of each process.

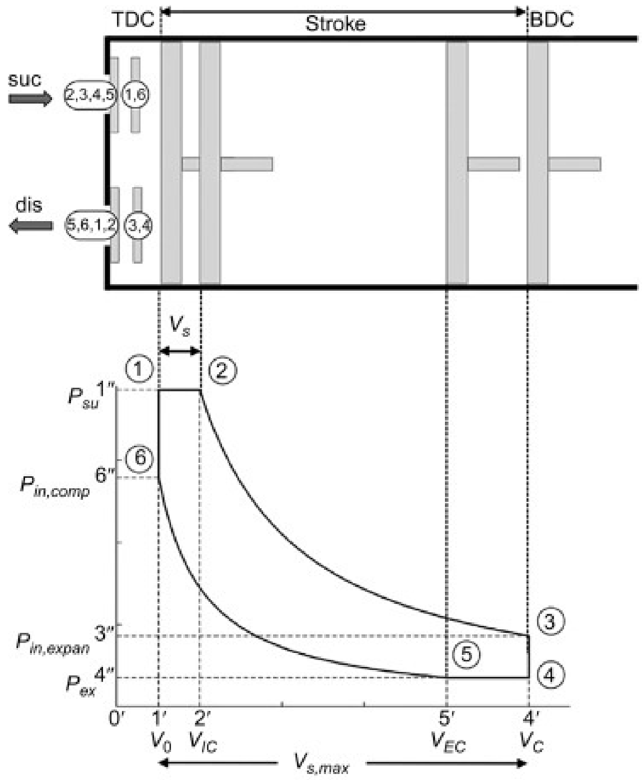

Figure 3: Pressure volume graph of Piston expansion process [3]

In the Simulink model for the Expander, the working fluid properties (which include-

Process number	description of working fluid
1-2	Working fluid admission at supply pressure
2-3	Expansion of working fluid
3-5	Discharge of working fluid from cylinder
5-6	Pressure increase of remaining working fluid

Table 2: Processes in a piston expander

pressure, enthalpy, phase, density and temperature) exiting the boiler, working fluid mass flow, condenser pressure and the rotational speed is given as an input and the model calculates the expander power and evaporator pressure. As a first step, the expander inlet density is calculated by the model as per equation 8. From Figure 3, COR is the ratio between V_{ic} and $V_{s,max}$

$$\rho_{wf,in} = \frac{\dot{m}_{wf}}{N_{exp}} \frac{1}{V_{exp} n_{exp} COR} \tag{8}$$

The density obtained from Equation 8 is used to calculate the evaporator pressure. As shown in Equation 9

$$P_{exp,in} = f(\rho_{wf,in}, T_{wf,exp\ in}) \tag{9}$$

Finally, for calculating the expander power, first, the entropy of working fluid at expander inlet is calculated and this entropy is again used to calculate the isentropic enthalpy at the expander outlet, as shown in Equation 10 & 11

$$S_{exp,in} = f(\rho_{wf,in}, T_{wf,exp\ in}) \tag{10}$$

$$h_{exp,out} = f(P_{exp,out}, S_{exp,in}) \tag{11}$$

Lastly, the expander power is given by Equation 14

$$P_{exp} = \dot{m}_{wf} \eta_{exp} (h_{exp,in} - h_{exp,out}) \tag{12}$$

Velocity Expander

Turbo expanders can run at higher speeds as compared to volumetric expanders, and are a good choice for a WHR system due to their compactness and high level of performance, even in part load operation.[5] [1].

Similar to the volumetric expander, the evaporator pressure is calculated in the turbine expander model. A semi-empirical formulation of the Stodola equation is used to link the mass flow rate of the working fluid and the pressure drop across the expander, given in Equation 13

$$\dot{m}_{wf} = K_{eq} \sqrt{\rho_{wf,exp,in} P_{wf,exp,in} \left(1 - \frac{P_{wf,exp,in}}{P_{wf,exp,out}}\right)^{-2}} \tag{13}$$

A section of a turbo expander is represented in Figure 4

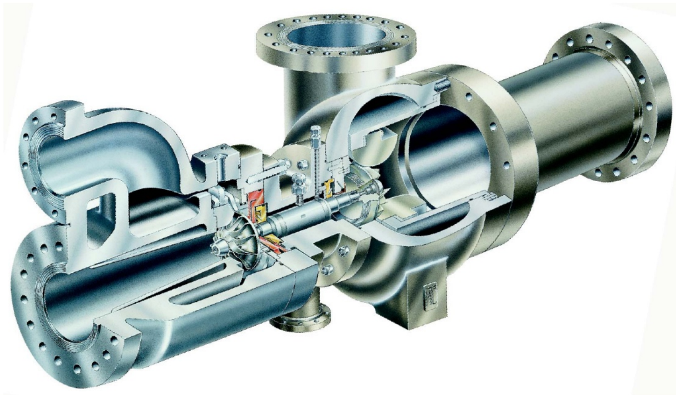

Figure 4: Section of a turbo-expander

2.2.2 Pump

Pump is a device to move liquid fluid in a circuit and increase its pressure. It causes fluid motion through mechanical action and the device requires power to operate.
A single cylinder reciprocating pump is used for this model, a schematic is shown in Figure 5. Working fluid mass flow in the system is calculated by the Equation 14

$$\dot{m}_{wf} = \rho_{pump,in} V_{pump,cylinder} N_{pump} \tag{14}$$

The pump power is calculated in the model using the given Equation 15

$$P_{pump} = \eta_{pump} \dot{m}_{wf} (h_{pump\ out} - h_{pump\ in}) \tag{15}$$

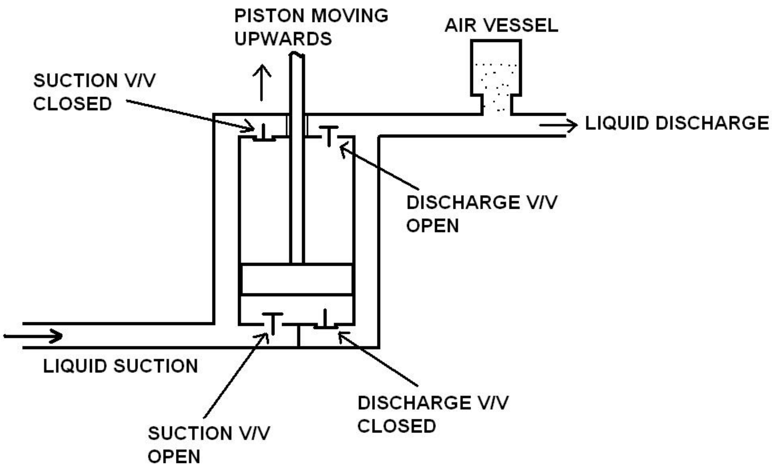

Figure 5: Reciprocating Pump Schematic

2.2.3 Evaporator

Evaporator and condenser are the two heat exchangers in the ORC. Hot and cold fluids are separated by a heat conducting surface and the property of heat to naturally flow from higher to lower temperature drives the heat transfer process. Conservation of mass and energy are the two principles which govern the heat transfer. Evaporator is responsible for the energy transfer from the hot source to the working fluid.Preheating, evaporation and super heating takes place in the evaporator.

Heat exchangers classification

Shell and tube type heat exchanger and plate and fin type heat exchanger are the two available choices for this application. Although shell and tube type heat exchanger offers an advantage of a smaller pressure drop in the fluid circuits, it is heavier and more space consuming as compared to plate heat exchanger. These are important criteria for for the heat exchanger in a marine vehicle. So, plate and fin type evaporator is selected. Heat is transferred from the hot side to the cold side by conduction as well as convection. Convection takes place in the two fluids and conduction takes place between the wall of the exchanger.

Heat exchangers can again be classified according to their flow configuration as either parallel flow or counter flow type. Figure 6 shows the schematic of temperature distribution along the two types of heat exchanger. A counter flow heat exchanger has been selected for modelling the evaporator and the condenser in the Simulink model. Counter flow type heat exchanger leads to higher heat transfer efficiency as compared to parallel flow type. This is because of a constant temperature difference between the hot and cold fluid in the counter current exchanger as compared with the parallel type. LMTD which is the driving force of heat transfer in the heat exchangers is higher in the case of counter current flow. And effect of entropy and irreversibility losses is also small in counter flow heat exchanger.

Choice of heat exchanger material

The material of the wall separating the two fluids in a heat exchanger is stainless steel. Even though, there are advantages of aluminium, like better thermal conductivity and lower cost, the advantages of stainless steel make it a better choice for wall material.

Advantages of stainless steel as wall material are

- Stainless steel resists corrosion in a wide range of pH levels, while aluminum will corrode if the proper fluids are not used to produce and maintain a narrow

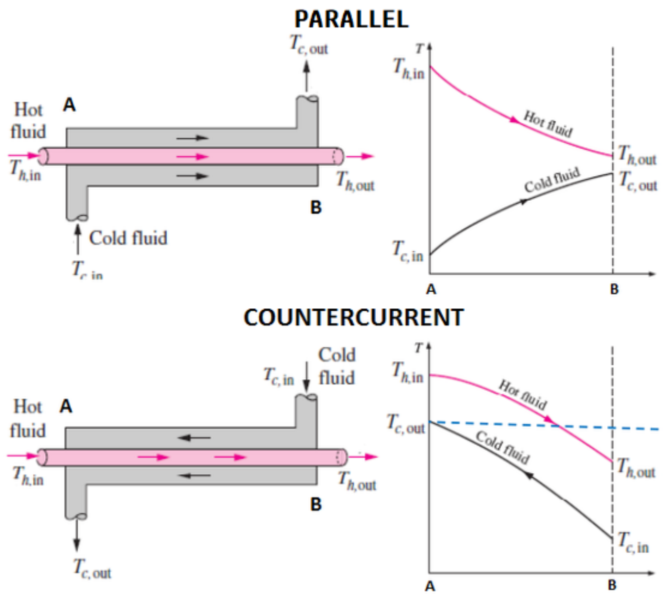

Figure 6: Types of heat exchanger

pH range.

- Aluminum heat exchangers require the use of special manufacturer recommended heat transfer fluids and inhibitors when starting up and maintaining the system

- Aluminum heat exchangers are also much more likely to suffer damage if not maintained at regular intervals.

- Aluminum can erode at high flow rates, while stainless steel heat exchangers operate very effectively at high flow rates

- Stainless steel heat exchangers are more expensive than aluminum, which is lightweight and has high thermal conductivity, but due to the longevity and corrosion resistance of stainless steel, they are likely to be a much better value in the long run.

Finite volume method

The model for the evaporator is a 1D finite volume model. The evaporator is descretized into N volumes along its length called control volumes. A single control volume is again divided into 3 parts, source fluid side, wall and working fluid side, as shown in Figure 7. Heat and mass balance ordinary differential equations are solved for each control volume, and integrated to give the total energy and mass transfer across the entire heat exchanger volume. The exchanger is descretized both in time and space, also called temporal descretizatoin. The equations given below represent calculation for node i, and the nodes on the left and right of i are represented by i-1 and i+1. The superscript on the variable " ' " represent the variable in a previous time step. Forward Euler method is used in the Simulink model to calculate the approximate solution of differential equations.

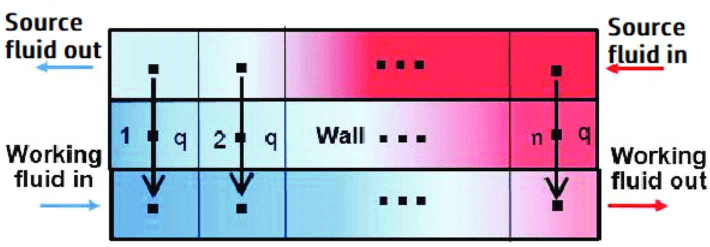

Figure 7: 1D finite volume heat exchanger

The mass balance equation in a control volume is given by Equation 16. The mass variation in time in each volume can be expressed by means of the differential of the enthalpy and pressure.

$$.\frac{dM_i}{dt} = V\frac{d\rho}{dt} = V(\frac{d\rho}{dh}\frac{dh}{dt} + \frac{d\rho}{dp}\frac{dp}{dt}) = m_i' - m_{i-1}' \tag{16}$$

The energy balance equation in a control volume is represented by Equation 17

$$\frac{dU_i}{dt} = m_{i-1}h_{i-1}' - m_ih_i' + Q_i + W_i - p\frac{dV}{dt} \tag{17}$$

Considering the work done in a control volume to be 0 and using the equation for internal energy,U=H-pV and considering p as constant in the direction of flow, the energy balance equation for the working fluid control volume is expressed by Equation 18

$$\rho_iV_i\frac{dh_i}{dt} = m_{i-1}'(h_{i-1}' - h_i') + m_{i-1}'(h_i' - h_i) + Q_i + V\frac{dp}{dt} \tag{18}$$

For the heat source side, the enthalpy can be written as a product of temperature and specific heat of the source fluid. The energy balance equation for heat source control volume is given by Equation 19

$$\rho_iV_iCp\frac{dT_i}{dt} = m_{i-1}'Cp(T_{i-1}' - T_i') - m_i'Cp(T_i' - T_i) + Q_i \tag{19}$$

The energy balance equation for the wall is given by Equation 20

$$M_w Cp_w \frac{dT_w}{dt} = Q_{source-wall} - Q_{wall-workingfluid} \tag{20}$$

The total heat transferred in the evaporator is expressed by Equation 21

$$Q_{evap} = U_{total} A_{total} \Delta T_{lm} \tag{21}$$

U_{total} and A_{total} are the global heat transfer coefficient and global heat exchange area respectively. T_{lm} is the log mean temperature difference between the two fluids. The amount of heat transferred on both sides of the evaporator wall can be expressed by Equation 22 & 23

$$Q_{source-wall} = U_{source} A_{source-wall} \Delta T_{source-wall} \tag{22}$$

$$Q_{wall-workingfluid} = U_{workingfluid} A_{wall-workingfluid} \Delta T_{wall-workingfluid} \tag{23}$$

Heat Transfer coefficient

The total heat transfer equation can be expressed as Equation 24

$$\frac{1}{U_{tot}} = \frac{1}{h_{hot_fluid}} + \frac{t_{wall}}{K_{wall}} + \frac{1}{h_{wf}} \tag{24}$$

In the model heat transfer coefficient,U is found out for the working fluid in each control volume using Dittius Boelter equation, Equation 25 for single phase heat transfer coefficient and Shah's correlation for two phase heat transfer coefficient, , Equation 26.

$$Nu = 0.023 Re^{0.8} Pr^{0.3} \tag{25}$$

$$Nu_{2\phi} = Nu_{sp} * \frac{(1-q)^{0.8} + (3.8q^{0.76}(1-q)^{0.04})}{P_{red}^{0.36}} \tag{26}$$

Reynolds number, Prandtl number, Nusselt number and reduced pressure ratio are expressed by Equation 27, 28, 29 & 30 respectively.

$$Re = \frac{\rho v l}{\mu} \tag{27}$$

$$Pr = \frac{\mu C_p}{k} \tag{28}$$

$$h = \frac{Nu\ k}{l} \tag{29}$$

$$P_{red} = \frac{P_{act}}{P_{critical}} \tag{30}$$

Phase of the fluid is calculated by Equation 31

$$q = \begin{cases} 0 & \text{if } h_{wf} \leq h_{liq,sat} \\ \frac{h_{wf} - h_{sat,liq}}{h_{sat,vap} - h_{sat,liq}} & \text{if } h_{liq,sat} < h_{wf} < h_{vap,sat} \\ 1 & \text{if } h_{wf} \geq h_{vap,sat} \end{cases} \tag{31}$$

Amount of superheat and subcooling of a working fluid at the expander and pump inlet respectively, is expressed in Equations 32 & 33. Here, $T_{sat,e}$ represent the vapour saturation temperature of the working fluid at the evaporator pressure & $T_{sat,c}$ is the liquid saturation temperature of the working fluid at condenser pressure.

$$T_{superheat} = T_{wf,exp,in} - T_{sat,e} \tag{32}$$

$$T_{subcool} = T_{sat,c} - T_{wf,pump,in} \tag{33}$$

The input to the evaporator model is the working fluid conditions at the pump exit, working fluid mass flow rate, evaporator pressure, source mass flow and flow rate. The model calculates the working fluid properties at the evaporator exit, source fluid exit temperature and total heat transfer in the evaporator.

2.2.4 Condenser

Condenser is a heat exchanger which is used to expel the heat from the working fluid in the ORC. The model for the condenser is also a 1D finite volume model, similar to the evaporator. Indirect condensation method is adopted for this model since it is used for marine application and sea water for cooling is available in abundance. Working fluid is condensed and sub cooled in the condenser. A pump is used to provide sea water to the condenser. The condenser pressure is determined by the sea water temperature, boiling point of the working fluid and the heat exchanger design. The condenser pressure is always maintained above atmospheric pressure to prevent the possibility of atmospheric air entering the working fluid circuit.

2.3 Controls

In a transient model, the objective of the control system is to ensure electricity production from the ORC with the most optimum cycle efficiency while ensuring safe operation. The operating limits of the equipment should not be exceeded such

as the pump and expander speed limits and the pre-determined pinch points of the exchangers. It is also the job of the control system to to prevent the entry of working fluids containing liquid and vapour phase in turbine and pump respectively.
A PID (Proportional Integral Derivative) controls are used for controlling the rankine system in this case. A simple schematic of a close loop PID controller is shown in Figure 8
P stands for proportional gain, the gain is proportional to the error value, which is expressed as SetPoint(SP)- Process variable (PV)
I term is the integral term, which accounts for the past values of errors. The errors are integrated over time. It helps the controlled variable to reach the setpoint value.
D term is the derivative term, its purpose is to reduce the overshooting from the setpoint due to the effects of the first two terms. Due to the coupled nature of the

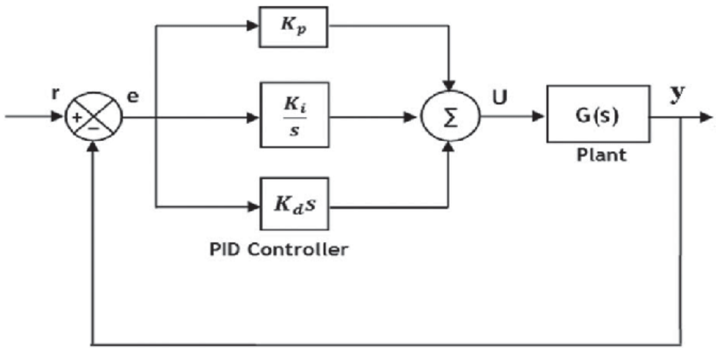

Figure 8: Schematic of closed loop PID controller

process, the control problem is generally complex.
A PID controller controls the speed of the sea water pump to ensure that the working fluid is subcooled to a set point $T_{subcool}$ in the condenser. Sub cooling does not benefit the performance of the ORC, the only reason for sub cooling is to have a margin/ buffer to prevent working fluid in the vapour phase to enter the pump during transient operation of the ORC. The sub cooling set point must be selected carefully since high set point value can result in decreased cycle efficiency.
Similarly, another PID controller, controls the evaporator pressure by changing the working fluid speed, to ensure a set temperature $T_{superheat}$ of super heat of the working fluid is maintained while entering the expander. Similar to the condenser control, the main purpose of keeping a superheat set point is to have a margin to ensure that the fluid is in complete vapour phase before entering the expander. Selection of the superheat temperature setpoint is important because, with higher setpoint, the working fluid mass flow reduces, resulting in lower cycle efficiency.
PID tuning was a very important activity for attaining fluctuation-free signal and

ensuring that the controller functions properly. A simple method used to find the static gain and time constant is shown in Figure 9. A change in one parameter (from N_0 to N) causes change in another parameter (SC_0 to SC) with a time delay, λ, required for 63% of change in SC. The static gain is given by Equation 34 and the Time constant is given by Equation 35, can be used to determine the P & I gains. For the first order models, SIMC (Skogestad Internal Model Control) method are very effective in PID tuning. Using this method the gain value and the time constant can be calculated. [11]

$$G = \frac{N - N_0}{SC - SC_0} \tag{34}$$

$$\tau = \lambda \tag{35}$$

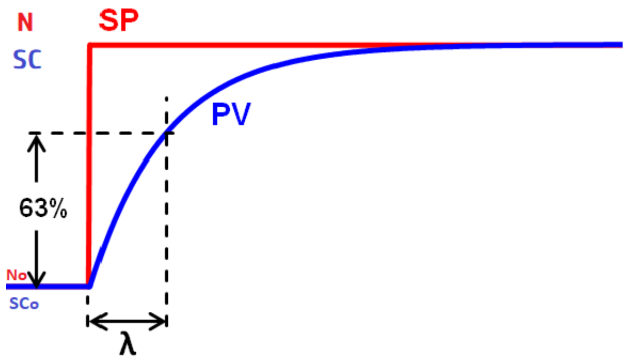

Figure 9: PID Tuning method

2.4 Fluid Selection

The important properties of the working fluid are mentioned below. Table 3.5 provides the properties of the fluid.

In the 1st screening of working fluids for the ORC, thermo-physical, safety and environmental parameters are compared. For this thesis, all the working fluids being considered are already existing in the market and not future refrigerants or one's currently in development. The properties being considered are mentioned below.

Type of fluid

The fluid can be classified into dry, wet and isentropic on the basis on the slope of

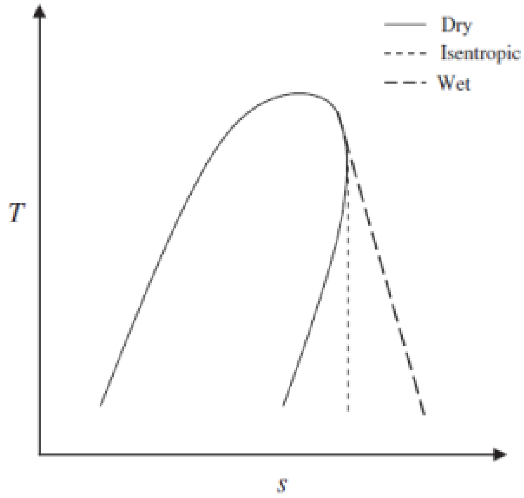

Figure 10: T-S diagram of dry, wet and isentropic fluids

their vapour saturation curve. As seen from Figure 10, Wet fluids have a positive slope, dry fluids have negative slope and isentropic fluid have 0 slope. This property is very important in case of rankine cycle application. Wet fluids have a disadvantage because in order for the phase of the fluid to be completely vapour throughout the expansion process, super heating the fluid be required. Dry fluids will always have pure vapour at the outlet of the expander, even if no super heating is done, because of the slope of the vapour curve.[9]

Boiling Point

Boiling point is an important criteria for deciding the working fluid. The source and sink temperature of the Rankine cycle determine the choice of the fluid with appropriate boiling point. If the boiling point is too high, then the heat source would not be able to boil the working fluid (that is why water is not considered in this case) and if the boiling point is too low (eg. R32) then the system would need to be highly pressurized, which comes with its own drawbacks.

Heat of vaporization

Having a high heat of vaporization is beneficial for the ORC, because it is inversely proportional to the refrigerant charge required. For this reason, cyclopentane with a heat of vaporization of 389 kJ/kg required only 0.15 kg/s of mass flow whereas

Working fluid	Chemical formula	Type	Boiling Point	Heat of vaporization	Specific heat	Thermal conductivity	Critical temperature	Critical Pressure	Viscosity	Density	Mol. weight	Global warming potential	Ozone depliton potential	Safety class	Cost
			$°C$	kJ/kg	kJ/kg.K	W/m.K	$°C$	bar	1e-3*Pa.s	kg/m^3	g/mol				£/kg
R1233zd	Trans-1-chloro-3,3,3-trifluoroprop-1-ène	Dry	18.31	195.35	1.243	0.077	165.6	35.75	0.469	1263	130.5	5	0	A1	33.29
R245fa	1,1,1,3,3 – PENTAFLUOROPROPANE CF3-CH2- CHF2	Dry	15.13	196.05	1.322	0.088	154	36.51	0.401	1339	134.05	1030	0	B1	49.31
R1234yf	2,3,3,3-tetrafluoroprop-1-ene	Dry	-29.4	180.25	1.392	0.064	94.7	33.81	0.154	1092	114	4	0	A2L	88.82
R134a	1,1,1,2 – TETRAFLUOROETHANE CF3-CH2F	Dry	-26.08	217	1.425	0.081	101.1	40.59	0.195	1207	102.03	1430	0	A1	12.74
Novec 649	CF3CF2C(O)CF(CF3)2	Dry	49	88	1.103	0.059	169	18.8	0.49	1600	316	1	0		119.5
R32	Di Fluoromethne CH2F2	Dry	-51.65	381	1.94	0.135	78.11	57.82	0.114	961	52	675	0	A2L	49.875
R454B	R-32(69.9%)(CH2F2)/R-1234yf(31.1%)(2,3,3,3-Tetrafluoropropene)	Dry	-50.9	352.98	1.444	0.1561	80	50.4	0.287	996.5	62.6	467	0	A2L	35.44
R1234ZE	Trans-1,3,3,3-tetrafluoroprop-1-ène	Dry	-19	195.6	1.386	0.0744	109	36	0.199	1163	114	6	0	A2L	31.21
R717	NH3	Dry	-33.5	1367	4.78	0.666	132.35	113	0.2564	682.29	17	0	0	B2	3.96
Cyclopentane	C5H10	Dry	49	389	1.935	0.118	238	44	0.319	716.117	70	25	0	A3	120.8
R1234ZE(Z)	Cis-1,3,3,3-tetrafluoropropene	Dry	9.745	195	1.217	0.0948	150.12	35.33	0.319	1260.04	114.04	1	0	A1	

Note. Heat of vaporization is calculated at the boiling point. Specific heat, thermal conductivity, Viscosity are calculated at $25°C$ liquid fluid. Cost of refrigerant is a rough estimate.

Novec 649 with a heat of vaporization of 88 kJ/kg requires 0.23 kg/s of flow rate, while operating in the same conditions. Small fluid flow rates leads to small equipment sizes and thus less investment cost is needed for the system.

Thermal Conductivity

Higher the thermal conductivity, higher is the heat transfer coefficient, a property beneficial for the rankine cycle as less heat transfer area will be required in the heat exchangers leading to cost savings in the equipment.

Critical temperature and pressure

These two set the operation limits for the sub critical ORC application. They should be high so that the system is operatable for high temperature heat sources.

Viscosity

Higher values of liquid viscosity increases pressure drop in both evaporators and condensers.As a result, suction pressure at the compressor inlet decreases, discharge pressure increases and the mass flow rate of refrigerant also decreases, followed by a reduction in system capacity. Hence the viscosity of the refrigerant should be as low as possible.

Density

The higher the density, the lower the specific volume and volumetric flow rate. Low volumetric flow is desirable to achieve smaller component and more compact machines. Low density fluids have high specific volume and need bigger components (heat exchangers and expander). A bigger component size leads to more expensive units and more costly systems. Furthermore, a high specific volume increases the pressure drop in the heat exchangers and needs higher pump work.

Ozone depletion potential

The ODP of a compound is defined as the ratio of the total amount of ozone destroyed by that compound to the amount of the ozone destroyed by the same mass of CFC-11. So, CFC-11 has an ODP of 1. ODP of a refrigerant should be as low as possible, preferably 0.

Global Warming Potential

The Global Warming Potential (GWP) of a greenhouse gas is its ability to trap extra heat in the atmosphere over time relative to carbon dioxide (CO_2). So, the GWP of CO_2 is 1. This is most often calculated over 100 years, and is known as the 100 year GWP. This number should be as small as possible to ensure sustainable operation. Its rare to find substances with low flammability and reactivity as well as low GWP. For a compound to be less flammable and toxic the compound should be stable in the atmosphere. And at the same time, GWP is high for compounds that are stable and can stay in the atmosphere for longer. [8]

Safety

Refrigerant safety class is described by a matrix as given in Figure 11. Toxicity and flammability are measured by this matrix. A good working fluid should have A1 safety class.

	Lower toxicity	Higher toxicity
Higher flammability	A3	B3
Lower flammability	A2	B2
No flame propagation	A1	B1

Figure 11: Safety characterization of working fluid

3 Method

This chapter presents the methodology followed during the course of the project. It begins with collecting engine data for the model. Then a description of the model development procedure is provided, beginning with a simple 0D model and gradually introducing complexities, until a final 1D model is developed.

3.1 About the engine

Volvo D13 1000 HP (735kW) engine is used in this project for building an ORC model. Figure 12 is an image of a marine D13 engine. It is a very versatile engine with applications ranging from marine as well as industrial use. It is a 12.8L, 6 cylinder in-line diesel engine. In this project the application of the engine is in a passenger transport ferry. The availability of waste heat in large quantities made the engine a suitable candidate for waste heat recovery application. By recovering waste heat from coolant as well as the engine exhaust, the engine efficiency can be increased and the specific fuel consumption can be reduced.

3.2 Data collection

Collecting information about the possible extraction points of the engine coolant system was the first task of the project. CAC LP, CAC HP, Engine jacket, GOC, EOC were identified as possible heat sources for the ORC. A simplified schematic of the coolant system is shown in Figure 13. Extraction of heat at multiple locations

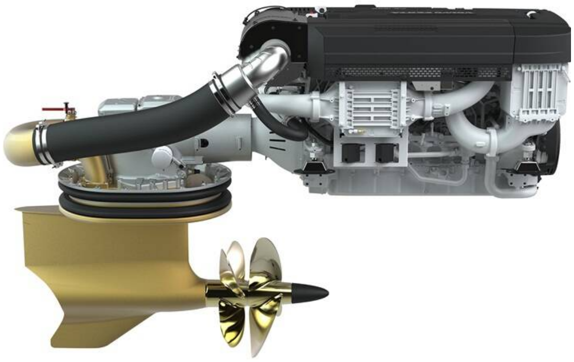

Figure 12: D13 engine

would require adding several heat exchangers in the engine cooling circuit and it will lead to excessive pressure drop in the ORC as well as the engine cooling system since the heat exchanger adds a considerable pressure drop to fluid circuits. With high pressure drop, the power consumed by engine coolant pump as well as ORC pump increases, which reduces the overall performance of the ORC. It also adds to the model complexity and cost of the system. It was decided to extract heat from one point in from the engine coolant system using a heat exchanger. The point right after thermostat was selected as the extraction point, since the coolant has the maximum temperature at this point.

From the engine test data, mass flow and temperature of engine coolant at the thermostat was collected for part load operation at different torque and speeds of the engine. Using this data, it was possible to map the source mass flow and temperature for a particular engine torque and speed.

A ”road cycle” is built to test the dynamic Simulink model from real engine data measured during testing of the boat. The information for the engine torque and speed are available from the test data at each second for a two hour long field test, as shown in Figure 14. This data is used in the Simulink model to determine the total energy generated from the ORC system in the road cycle. It can be seen that the engine speed and torque is highly transient in nature. The test cycle is obtained for a boat which transports passengers between two islands. During the test cycle, the Roll-on Roll-off (Ro-Ro) boat makes a number of return trips.

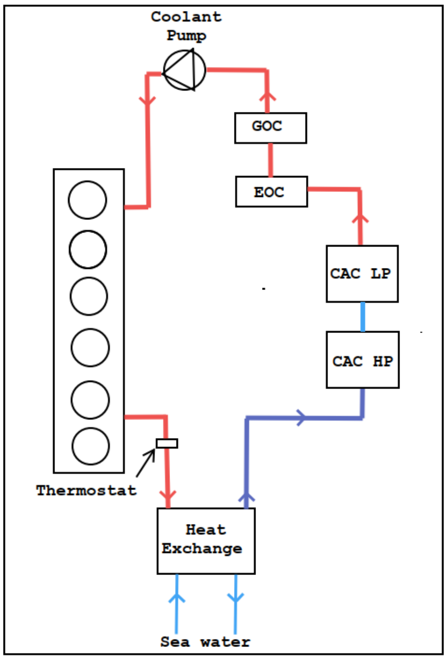

Figure 13: Schematic of coolant system in D13 engine

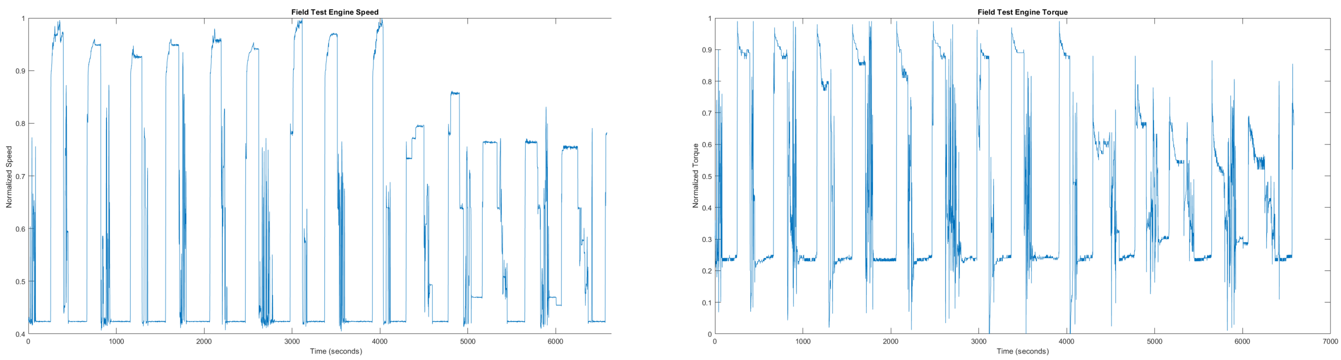

(a) Engine Speed

(b) Engine Torque

Figure 14: Field Test Data for Engine Speed and Torque.

3.3 Coolprop

The thermodynamic properties of all the refrigerants used in this project were taken from Coolprop database. It is an online open-source C++ library with a database of over one hundred pure fluids and mixtures. The fluid models implemented in CoolProp are based on Helmholtz energy formulation. The Coolprop extension can be easily added to MATLAB as an add-in. 1D and 2D lookup tables are created through MATLAB, which are used in the Simulink model. Liquid and vapour saturation temperatures, densities and enthalpies are found for different pressures. Similarly, temperature, entropy, density are found for different combinations of pressure and enthalpies.

3.4 0D model

In the beginning, a simple 0D model of the ORC is built using MATLAB and Coolprop with known source and sink data as well as working fluid properties. In Figure 15, a temperature-entropy diagram representing the waste heat recovery process as well as depicting the source and sink fluids. In a 0D model, basic thermodynamic equations are used to determine the heat duty of the exchangers and the power produced and consumed by the expander and pump respectively. The advantage of 0D model is its simplicity and small simulation time. The disadvantage of 0D model is a lack of accuracy and detail in the results as compared to a 1D model. The purpose of building a 0D model is to obtain a preliminary estimate of the results which can be expected from the Simulink model. Another reason for building a 0D model is that it allows further screening of refrigerants based on their performance for the given source and sink temperature ranges. Some key points of the 0D model are mentioned below-

- Input to the model is given as per Table 4.
- The model is not dynamic and represents only steady state calculation.
- No pressure drop was considered in the heat exchangers.
- Heat exchanger design wasn't considered. No restriction on the heat transfer area of the exchangers were imposed.
- Isentropic efficiency of the pump and the expander were considered as 70% and 60% respectively.

- Sink temperature is considered as 15 $°C$ as it is the average summer temperature of sea water near Gothenburg, Sweden.

- The evaporator and condenser pressure are fixed by the temperatures of the source and the sink. 5 $°C$ of pinch and 5 $°C$ of super heat is considered in the evaporator. And 7 $°C$ of sub cooling and 5$°C$ of pinch is considered in the condenser.

- The temperature of source fluid at the point where evaporation of working fluid ends is determined. Then the mass flow of the working fluid is calculated in the model, by the heat transfer equation between the source fluid and the working fluid.

- From known temperatures and pressures points, enthalpy,entropy and density of the working fluid can be calculated with which exchanger duties and expander and pump power can be determined.

- The MATLAB code used for 0D calculation is in Appendex of the report.

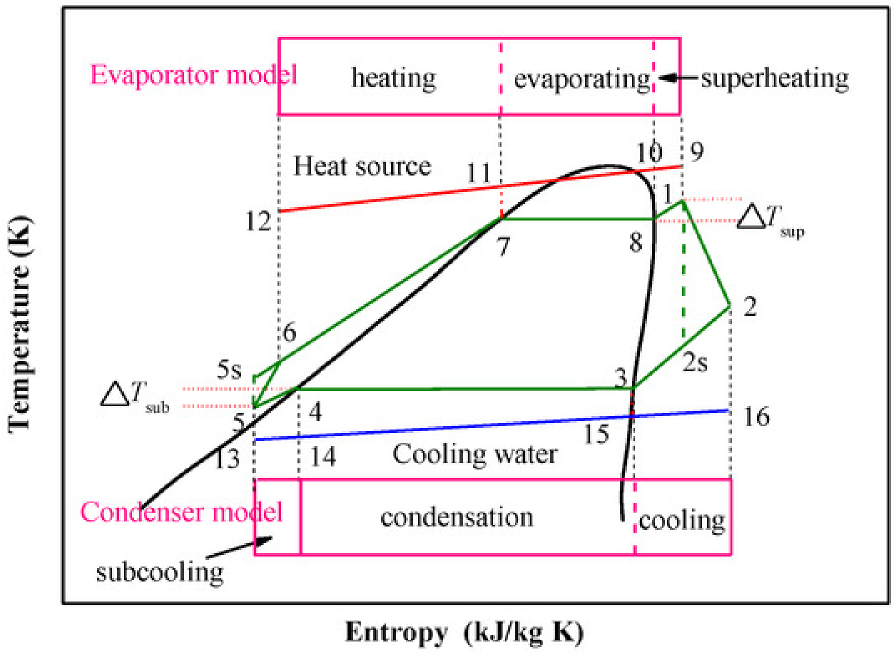

Figure 15: T-S diagram of an ORC system in a WHR process

3.5 Fluid Selection

From the list of fluids provided in Table , Cyclopentane, Novec 649, R1234yf, R1234ze(Z) were selected for the ORC model. These fluids showed good thermodynamic performance in the 0D models. They also had favourable physical properties like critical temperature & pressures and boiling points. The selected fluids also have good environmental properties and most of them are very safe for operation.

3.6 Aspen Model

In order to validate results of the 0D model and 1 D model, a similar model was made using Aspen Plus software, represented in Figure 16. It is built using the same input as Table 4 . Complex and accurate thermodynamic models can be built and simulated in this software. Aspen plus has a large database of fluids and very precise techniques for calculation of fluid properties and thermodynamic processes.The software also has a rich database of costs of mechanical components such as the ones used in this project.

A rankine cycle was modelled in the software, and considering the same parameters as the 0D model. All the different refrigerants were tried in this model, except for R1234ze(Z) as its data wasn't available in Aspen.

The models are also used for a rough capital cost estimate of the entire system using the Economic analyser function of the software.

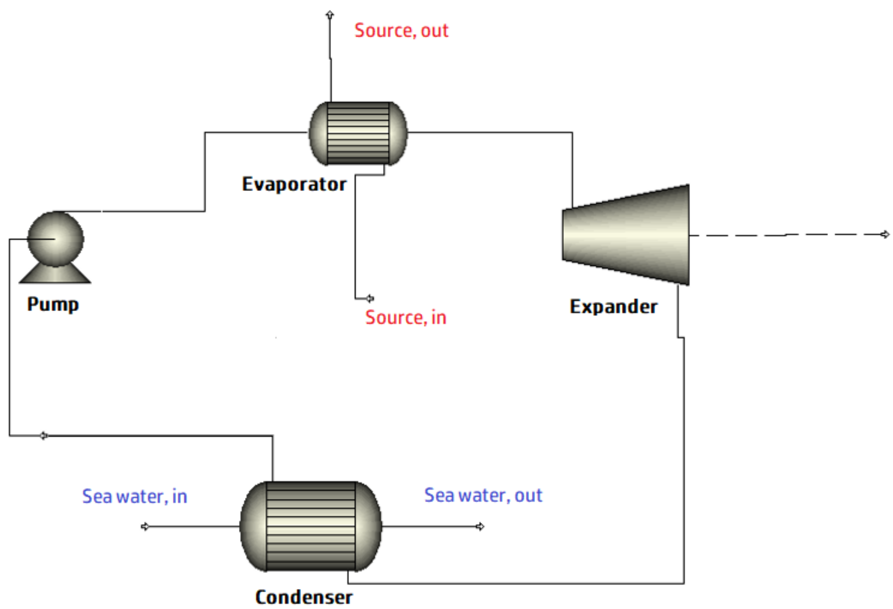

Figure 16: Aspen model

3.7 1D Simulink model

Each component of the model is developed separately using the concepts form Chapter 2. Figure 18 is an image of the Simulink model. Then the components are connected together and the model is run for constant values of evaporator and pumps speeds and constant source input. The results are examined to see if the signals are fluctuating or an unexpected value occurs. Then the PID controls are introduced to manipulate the speed of the sea water pump and the working fluid pump as per the specified set point. The performance of the model is checked for steady state input conditions. The input is the same as 0D and Aspen Plus model, as per Table 4.
After the steady state operation, the model is fed transient input data for the "road cycle". The performance of different refrigerants in the same road cycle are compared.
For transient operation, tuning the PID controllers that control the speed of working fluid pumps and sea water pumps is very important. Figure 17 shows the variation of subcooling value throughout the operation cycle. The sea water pump speed is varied to control the value of subcooling of the working fluid at the condenser exit. Tuning the PID controller was a challenging task due to non-linearity of the model and inter dependency on other PID controller. Before the PID contrller was tuned, it's was very sensitive and the signal was highly fluctuating. By reducing the P & I gains, the signal is made more stable with a small deviation from the set point value of sub cooling. Other PID controllers in the models ware tuned in a similar way.

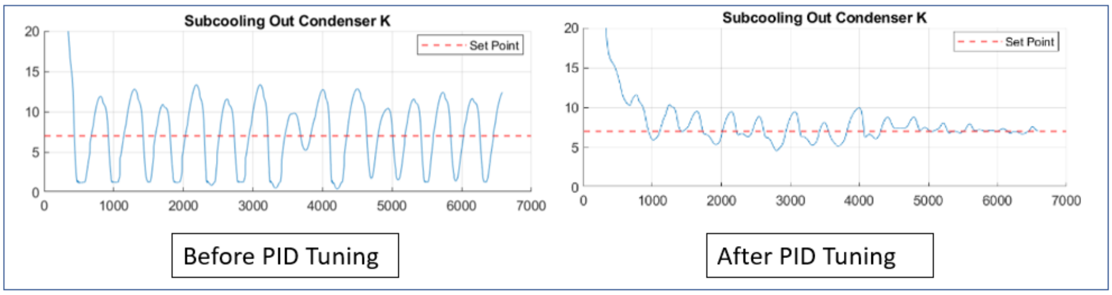

Figure 17: Signal Improvement

A number of assumptions are made in the Simulink model which could cause a possible deviation of the obtained output from the true output. These assumptions are mentioned below.

- No pressure drop occurs in the evaporator and condenser
- In the volumetric expander model, a constant cutoff ratio of 0.25 for piston cylinder expanders is used.

- The volumetric expander speed was considered a constant in this model and set as 5000 rpm. [15]

- In the Velocity expander model, the empirical value of K_{eq}, equation 13, is calculated considering a constant working fluid vapour density.

- The turbine expander speed was also considered constant in the model and kept as 22000 rpm. [7]

- For steady state performance calculation, results of which are provided in Figure 21, volumetric expander is used. And for dynamic performance evaluation, volumetric as well as velocity type expanders are used.

- Only convection is considered for fluid heat transfer. The effect of conduction in the heat transfer by the fluid is neglected.

- Constant heat transfer coefficient for source water and sea water are considered. And these fluids are considered to be only in their liquid phase in the model.

- Impact of the ORC system on the engine coolant pump power and the coolant sea water pump is not accounted in the model

- Lubrication oil for the expander is assumed to have no effect on the ORC performance.

- Mass flow of source fluid is calculated indirectly from the available data about the engine.

- Steady state test data of source temperature and mass flow are modified to fit the model for transient operation. The rate of change of the source mass and its temperature are limited in order to introduce the effect of inertia in the system. The input signals to the Simulink model obtained as a result, depicted the transient operation of the system more accurately.

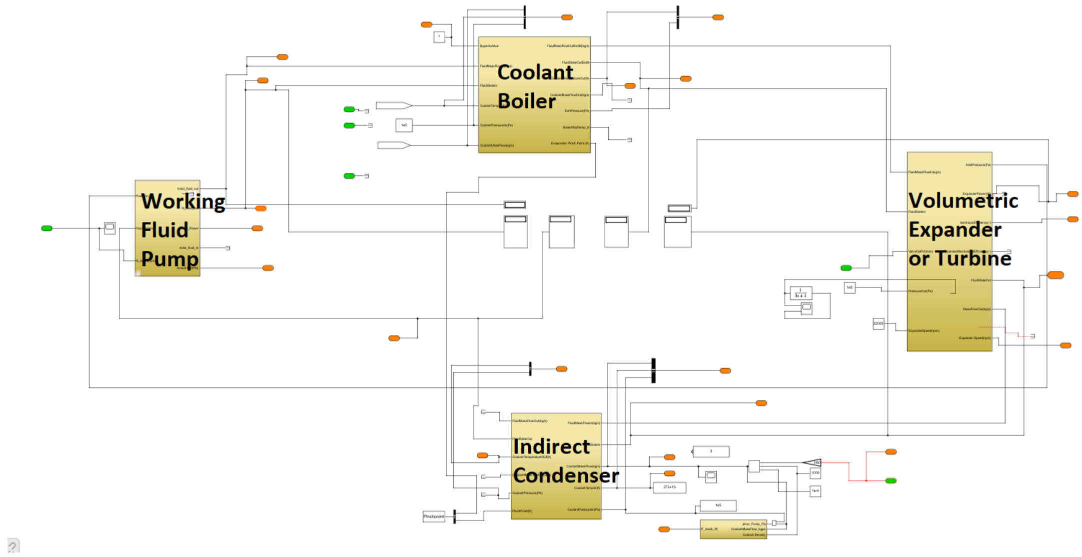

Figure 18: Simulink Plant model

Calculation procedure in Simulink model

The pump model obtains the input of working fluid properties from the condenser model. These properties are pressure, enthalpy, density, temperature and phase. It calculates the properties at the pump outlet. Each component calculates the fluid properties at the exit of the component, and these fluid properties are the inputs for the next component. In the pump model, working fluid mass flow rate is determined as well as the pump power. In the expander, the evaporator pressure is determined and the expander power. And in both the heat exchangers, the heat transfer between the two interacting fluids is found out. The same evaporator plate heat exchanger area, expander and pump volumes are used for each model.

4 Results

4.1 Steady State Results

First, a comparison between the Aspen Plus model and 1D steady state is done. Volumetric expander is used for the Simulink model in this case. Both models are given the same inputs, as shown in Table 4 and the result for expander power-Working fluid pump power is compared. From Figure 19,it can be seen that both models give similar outputs when they are provided with the same inputs. The slight deviation in the results could arise due to the difference in the heat transfer calculation in the Simulink model and the Aspen model. Another source of deviation can be the slight inaccuracies in the fluid properties lookup table for the Simulink model. It can also be deduced that R1234yf performs the best in this steady state application. It is also important to note that, in the figure, power refers to Expander power - Pump power. This is because, the sea water pump was not modelled the Aspen plus model.

Parameters	Units	Cyclopentane	Novec649	R1234yf	R1234ze(Z)
Source Mass flow	kg/s	2	2	2	2
Source Temperature	$^{\circ}C$	85	85	85	85
Sink Temperature	$^{\circ}C$	15	15	15	15
Working fluid mass flow	kg/s	0.15	0.23	0.66	0.26
Evaporator Pressure	bar	2.2	2.6	22	7.75
Condenser Pressure	bar	1.05	1.05	9.64	2.23
Turbine efficiency	%	60	60	60	60
Pump efficiency	%	70	70	70	70

Table 4: Steady state Inputs

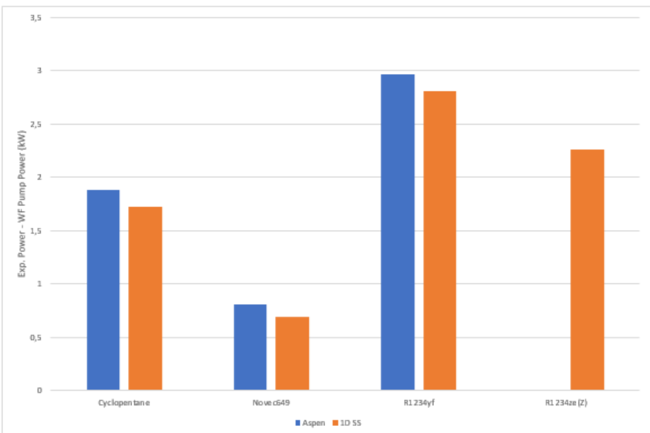

Figure 19: Net Power calculation through different methods

4.2 Dynamic Results

The models for all the four refrigerants were run on the road cycle which was created. The road cycle is about 1.8 hours with highly fluctuating engine speeds and torque. The graphs of results from the Simulink model of R1234ze(Z) with volumetric expander are shown in Figure 20 and the remaining models are shown in the Appendix.

In Figure 20, it can be seen that due to continuously varying heat source mass flow and temperature input to the model, the rest of the signals also adapt accordingly. When the heat source charge reduces, the evaporator pressure and the working fluid flow rate reduces. It also leads to reduced power of the expander and both pumps. The figure also shows that, the controller for super heating is better tuned as compared to the controller for sub cooling as it has a greater maximum deviation from the set point. The subcooling and superheating in the model is controlled by varying the speed of sea water and working fluid pumps respectively. The expander speed is considered constant for this model, for simplicity.

Another important observation is the difference between the turbine model and volumetric expander model outputs. After comparing the two, it can be seen that the evaporator pressure calculated in the turbine model is slightly lower as compared to the volumetric expander model (for the same refrigerant). As a result, the mass flow in the turbine model is higher than the volumetric expander model and subsequently, the expander power. This shows that lower evaporator pressure leads to higher working fluid mass flow rate, which results in higher net power of ORC.

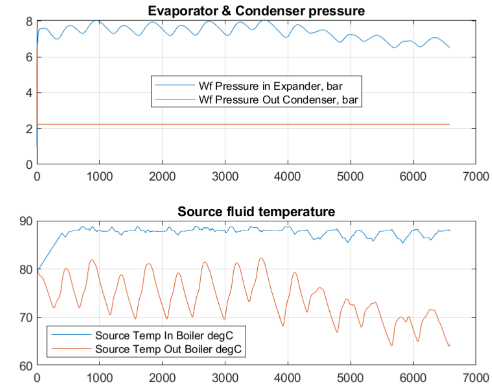

(a) Source temperature and Pressures

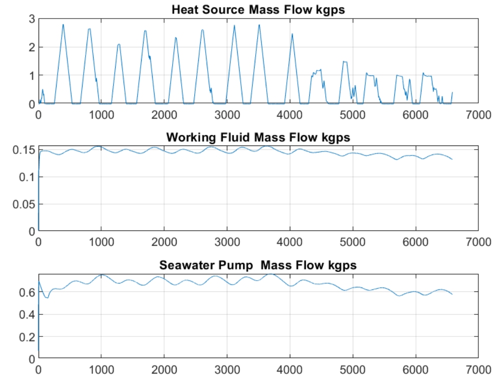

(b) Mass flow rates

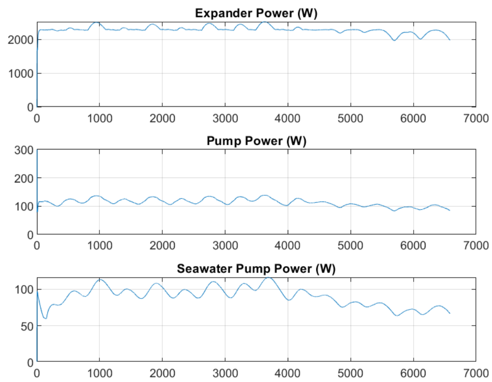

(c) Powers

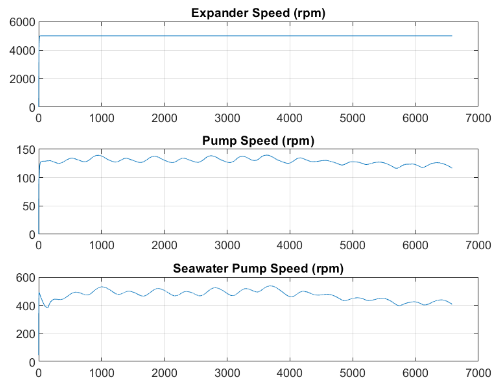

(d) Speeds

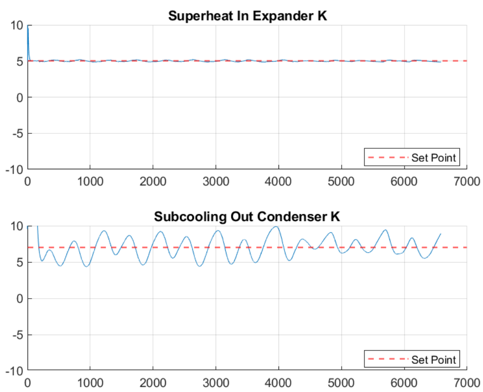

(e) Superheating and subcooling

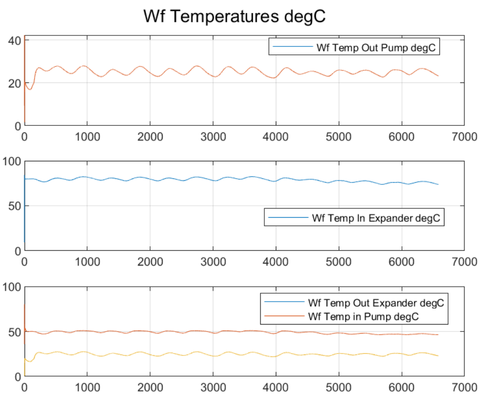

(f) Working fluid temperature

Figure 20: Dynamic simulation results for R1234ZE model with Volumetric Expander.

The total energy produced by the ORC over the cycle is shown in Figure 21. It can be seen that R1234ze(Z) gives the best results,for both types of expanders. And the higher performance of the Turbine expander as compared to the volumetric expander can also be seen from the Figure. It is also important to note that, even though the expander power of R1234yf model is greater than R1234ze(Z), the latter shows better overall performance. This is due to the high working fluid and sea water pump power requirement for R1234yf, since it operates on higher pressure levels of condenser and evaporator, as compared to the other fluids.

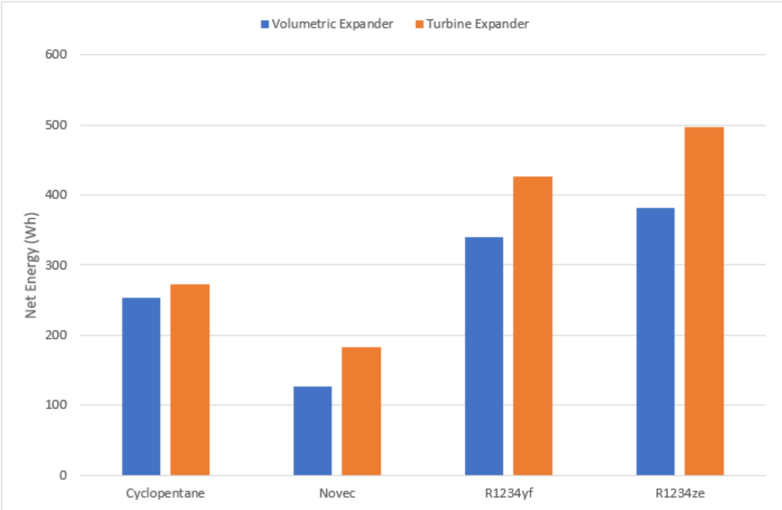

Figure 21: Total energy produced by the ORC in the road cycle

4.3 Economic Estimation

Figure 22 compares the investment cost in the Rankine system with the three different refrigerants. R1234ze(Z) couldn't be added to this comparison as the fluid data was not present in Aspen Plus. Pump is mapped as standard Ext gear rotary pump, Turbine as Turbo expander, Evaporator and condenser as U tube shell and tube heat exchanger. Table 5 and Table 6 show the equipment cost and installation cost of all the components in the ORC system.

It should be noted that there are a number of assumptions in the cost calculation of the system and the result of the cost should only be taken for the purpose of an estimate.

- Cost data of Aspen might not be accurate for this application.
- Only the 4 component are considered for the economic analysis. In reality other components like sea water pump, recuperator, filtration/ dosing system for the sea water pump, would also be included.
- Operating cost has to be considered for determining the pay back period, since replacing the refrigerant and oil with fresh fluid in ORC system would be costly.

The maintenance cost is also not considered.

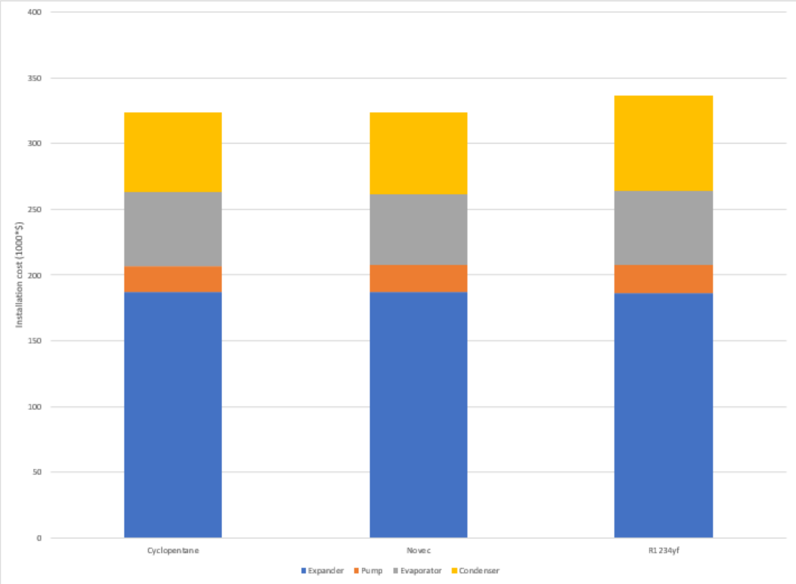

Figure 22: Installed equipment cost of ORC with different refrigerants

It can be observed from the Figure 22 that the installation cost for the three different refrigerant systems is quite similar, with R1234yf being slightly higher. It can also be observed that the expander cost is the major cost of an ORC system. The higher cost of R1234yf ORC can be attributed to higher heat exchanger cost. Another scenario was evaluated for cost, where the mass flow rate of source, sea water and the working fluid was made 10 times, to see how the investment costs would change if the heat source was scaled 10 times. The higher flow rates also resulted in ten times higher Net power output from the ORC. It can be seen from the Figure 23

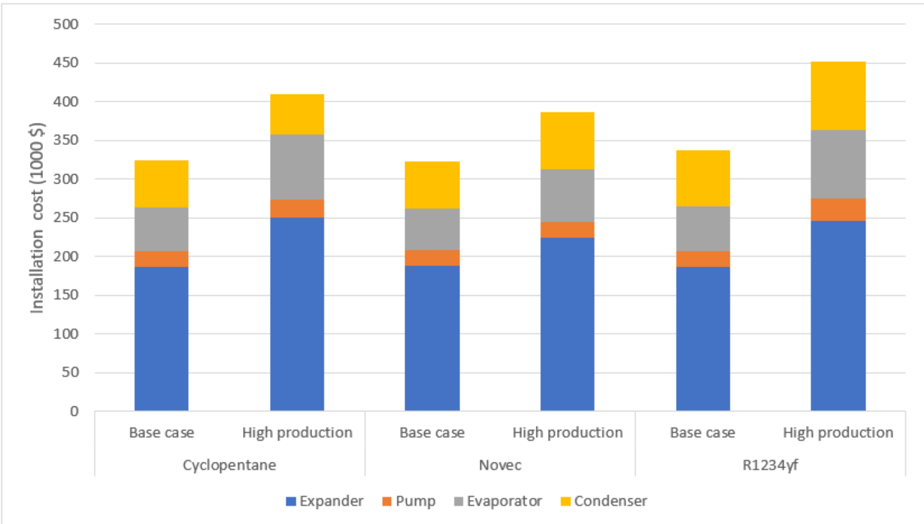

Figure 23: Cost comparison between base case and high production case

that even though there is an increase in the investment cost for high production scenario, it is still small as compared to the increase in the output. This shows that the machine will be more and more cost effective for higher flow rates.
Using a fixed cost price of electricity, and a specific fuel consumption value of the on-board diesel generator set, the annual cost saving from the ORC system can be calculated. Considering 2$/litre as the fuel cost and assuming 6000 hrs of annual operation of the boat, it was calculated that the installation cost of the ORC system can be recovered in 19.5 years for the base case and in 2.3 years for the high production scenario, (for R1234yf refrigerant model). This proves that the WHR system can becomes more commercially viable with larger scales.

5 Discussion

The following are the important learnings from the project.

- R1234ze(Z) is a safe and environment friendly refrigerant which gives very good thermodynamic performance in a low grade WHR system. 500 Wh of energy is produced by the R1234ze(Z) ORC model with turbo expander over a duration of 1.8 hour of operation. The ORC efficiency is the maximum for R1234ze(Z) refrigerant model, 6.5% which means that the system is able to recover 6.5% of the coolant waste heat.

- In condenser, the sub cooling setpoint is set higher than super heating setpoint. This is because, super heating is controlled directly by the working fluid pump and the sub cooling is controlled indirectly by the sea water pump as there is a time delay in the response of the sub cooling of the working fluid and the mass flow of the sea water, as they are two different circuits.

- The expander power depends on the working fluid mass flow and the pressure ratio between expander inlet and outlet. For a fixed source and sink temperature, an increase in pressure ratio results in a decrease in mass flow of the working fluid. There exists an optimum pressure ratio which gives the maximum expander power.

- R1234yf has higher expander power than R1234ze(Z) but due to its higher working fluid pump power, the overall net power is lower. The reason for its high working fluid pump power is due to the high evaporator and condenser pressure of the system.

- There is no ideal refrigerant which is suitable for all ORC application. The choice of working fluid depends heavily on the application and the source and sink temperatures. Depending on where the ORC is used, the concerned property of the fluid becomes critical. For example, in a marine application, environmental and operational safety aspects are very important and thus, they determine the selection of the working fluid.

- The pay back period of the ORC system reduced from 19 years to 3 years on increasing the scale of the system by ten times. This shows that the ORC system becomes a more cost effective solution for large scales waste heat recovery.

5.1 Future Work

Due to time constraints, there were a few interesting activities/experiments which could not be done. These activities are listed below.

- Seeing the effect of refrigerant mixtures since refrigerant mixtures perform better than pure fluids when source conditions vary.

- Include the engine exhaust as a heat source for the ORC along with the engine coolant system.

- Compare the performance of the ORC with and without a recuperator.

- Modelling the effect of the lubrication oil on the performance of the ORC. Instead of pure fluid, considering the working fluid as a mixture of refrigerant and expander lubricant oil and calculating the thermal properties of the mixture for different operating points accordingly. And these thermal properties will be used in the Simulink model.

- Experimental validation of the model on a test rig.

6 References

[1] Fuhaid Alshammari, Apostolos Karvountzis-Kontakiotis, Apostolos Pesyridis, and Muhammad Usman. Expander technologies for automotive engine organic rankine cycle applications. *Energies*, 11(7):1905, 2018.

[2] SE Aly. Diesel engine waste-heat power cycle. *Applied Energy*, 29(3):179–189, 1988.

[3] Paul Breeze. *Combined heat and power*. Academic Press, 2017.

[4] V Dolz, R Novella, A García, and J Sánchez. Hd diesel engine equipped with a bottoming rankine cycle as a waste heat recovery system. part 1: Study and analysis of the waste heat energy. *Applied Thermal Engineering*, 36:269–278, 2012.

[5] Nicolas Espinosa. *Contribution to the study of waste heat recovery systems on commercial truck diesel engines*. PhD thesis, Université de Liège-INPL Nancy, Liège, Belgique, 2011.

[6] Yuh-Ren Lee, Chi-Ron Kuo, and Chi-Chuan Wang. Transient response of a 50 kw organic rankine cycle system. *Energy*, 48(1):532–538, 2012.

[7] KG Nithesh and Dhiman Chatterjee. Numerical prediction of the performance of radial inflow turbine designed for ocean thermal energy conversion system. *Applied Energy*, 167:1–16, 2016.

[8] Jamal Nouman. Comparative studies and analyses of working fluids for organic rankine cycles-orc, 2012.

[9] Khaled Senary, Adel Tawfik, Elsayed Hegazy, and Amr Ali. Development of a waste heat recovery system onboard lng carrier to meet imo regulations. *Alexandria Engineering Journal*, 55(3):1951–1960, 2016.

[10] Patrizia Serra and Gianfranco Fancello. Towards the imo's ghg goals: A critical overview of the perspectives and challenges of the main options for decarbonizing international shipping. *Sustainability*, 12(8):3220, 2020.

[11] Mohammad Shamsuzzoha and Sigurd Skogestad. The setpoint overshoot method: A simple and fast closed-loop approach for pid tuning. *Journal of Process control*, 20(10):1220–1234, 2010.

[12] T. W. P. Smith, J. P. Jalkanen, B. A. Anderson, J. J. Corbett, J. Faber, S. Hanayama, E. O'Keeffe, S. Parker, L. Johansson, L. Aldous, C. Raucci,

M. Traut, S. Ettinger, D. Nelissen, D. S. Lee, S. Ng, A. Agrawal, J. J. Winebrake, M. Hoen, S. Chesworth, and A. Pandey. *Third IMO Greenhouse Gas Study 2014*. International Maritime Organization, United Kingdom, April 2015.

[13] Bertrand F Tchanche, Pierre Loonis, Mathieu Pétrissans, and Harry Ramenah. Organic rankine cycle systems principles, opportunities and challenges. In *2013 25th International Conference on Microelectronics (ICM)*, pages 1–4. IEEE, 2013.

[14] Iacopo Vaja and Agostino Gambarotta. Internal combustion engine (ice) bottoming with organic rankine cycles (orcs). *Energy*, 35(2):1084–1093, 2010.

[15] EH Wang, HG Zhang, Y Zhao, BY Fan, YT Wu, and QH Mu. Performance analysis of a novel system combining a dual loop organic rankine cycle (orc) with a gasoline engine. *Energy*, 43(1):385–395, 2012.

7 Appendix

7.1 0D model Matlab code

0D model for ORC

```
clc;
clear all;
Fluid_name='R1234ze(Z)';
T1=85;%in $^{\circ}C$
T_HX_Pinch=5;%in K
M1=2;%in kg/s
Eff_T=0.6;%in %
Eff_P=0.7;%in %
Cp=4.18;%in kJ/kg.K
Super_heat=5;%in K
Sub_cool=7;%in K
T_SW_In=15;%in $^{\circ}C$
M_SW=1.2;%in kg/s
P_Pa=101325;%in Pa
T_K=273;%in K
j=30;%number of parts
i=7.55; %pressure in bars
P1=i*P_Pa; %in Pa, evaporator pressure
P2=2.236*P_Pa; %in Pa, condenser pressure
T_evap=py.CoolProp.CoolProp.PropsSI('T','P',P1,'Q',0,Fluid_name)-T_K;%in $^{\circ}C$
T_cond=py.CoolProp.CoolProp.PropsSI('T','P',P2,'Q',0,Fluid_name)-T_K;%in $^{\circ}C$
h_wf_evap_sup_vap=py.CoolProp.CoolProp.PropsSI('H','P',P1,'T',T_evap+T_K+Super_heat,Fluid_name)*0.001;%in KJ/kg
```

```
s_wf_evap_sup_vap=py.CoolProp.CoolProp.PropsSI('S','P',P1,'T',T_evap+T_K+Super_heat,Fluid_name);%in J/kg.K
h_wf_evap_sat_liq=py.CoolProp.CoolProp.PropsSI('H','P',P1,'Q',0,Fluid_name)*0.001;%in KJ/kg
h_wf_cond_sat_vap=py.CoolProp.CoolProp.PropsSI('H','P',P2,'S',s_wf_evap_sup_vap,Fluid_name)*0.001;%in KJ/kg
h_wf_cond_sat_liq=py.CoolProp.CoolProp.PropsSI('H','P',P2,'T',T_cond+T_K-Sub_cool,Fluid_name)*0.001;%in KJ/kg
Q1=M1*Cp*(T1-(T_evap+T_HX_Pinch));%in kW
m_wf=Q1/(h_wf_evap_sup_vap-h_wf_evap_sat_liq);%in kg/s
W_exp=m_wf*Eff_T*(h_wf_evap_sup_vap-h_wf_cond_sat_vap);%in kW
W_pump=m_wf*Eff_P*(P1-P2)*0.001/py.CoolProp.CoolProp.PropsSI('D','P',P2,'Q',0,Fluid_name);%in kW
W_net=W_exp-W_pump;%in kW
h_wf_before_evap=(W_pump/m_wf)+h_wf_cond_sat_liq;%in kJ/kg
T_wf_before_evap=py.CoolProp.CoolProp.PropsSI('T','P',P1,'H',h_wf_before_evap*1000,Fluid_name)-T_K;%in $^{\circ}C$
Q_tot_boiler=m_wf*(h_wf_evap_sup_vap-h_wf_before_evap);%in kW
T_out_water=T1-(Q_tot_boiler/(M1*Cp));%in $^{\circ}C$
Q_cond=m_wf*(h_wf_cond_sat_vap-h_wf_cond_sat_liq);%in kW
T_SW_out=T_SW_In+(Q_cond/(M_SW*Cp));%in $^{\circ}C$
```

7.2 ORC system cost

	Equipment Cost (in $)		
	Cyclopentane	**Novec 649**	**R1234yf**
Expander	86700	86000	87900
Pump	3400	3400	3450
Evaporator	11200	9400	14100
Condenser	9100	8900	11900
Total	110400	107700	117350

Table 5: Equipment Cost of ORC system

	Installation Cost (in $)		
	Cyclopentane	**Novec 649**	**R1234yf**
Expander	186900	187400	186700
Pump	20300	20300	20800
Evaporator	55700	53600	56700
Condenser	60600	61900	72300
Total	323500	323200	336500

Table 6: Installation Cost of ORC system

7.3 Dynamic Simulation Results

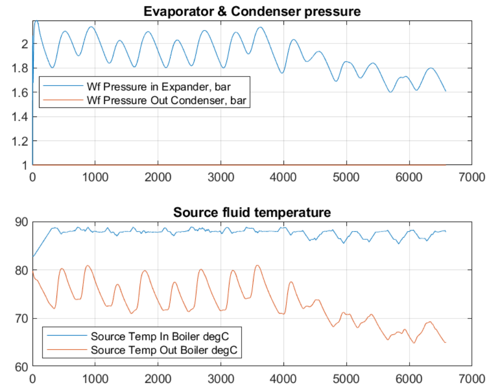

(a) Source temperature and Pressures

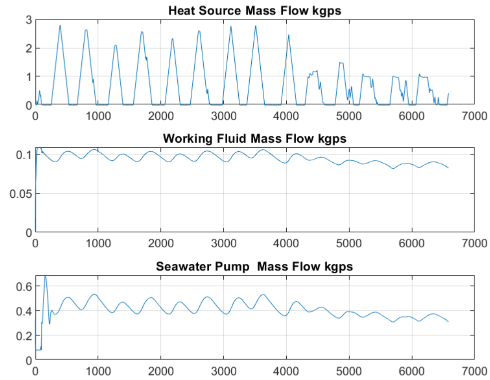

(b) Mass flow rates

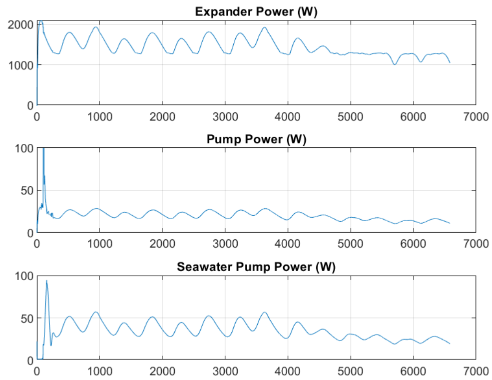

(c) Powers

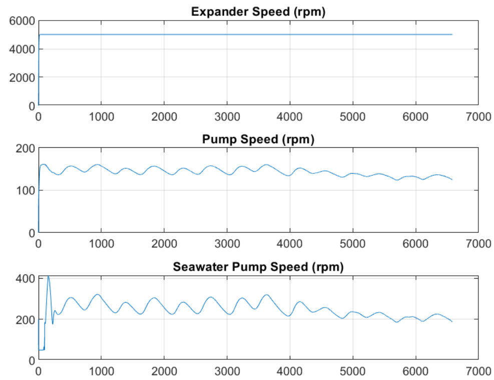

(d) Speeds

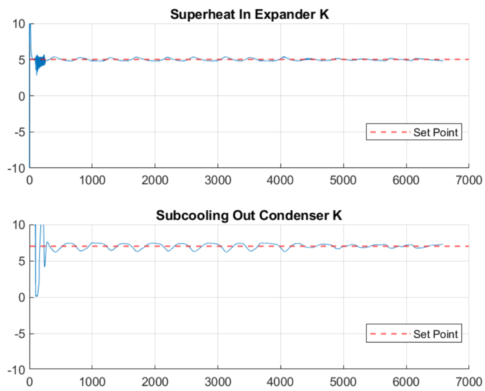

(e) Superheating and subcooling

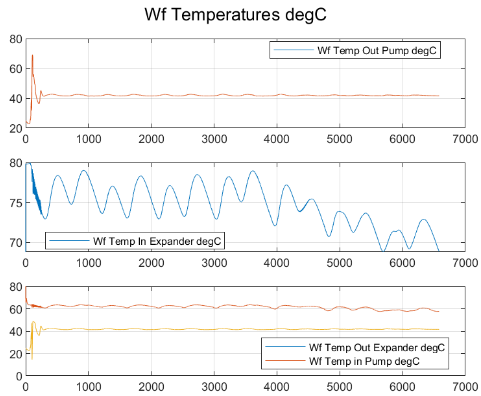

(f) Working fluid temperature

Figure 24: Dynamic simulation results for Cyclopentane model with Volumetric Expander.

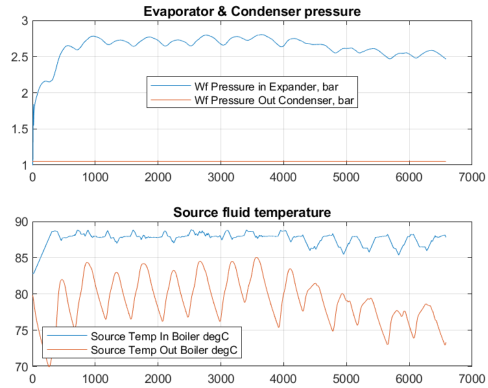

(a) Source temperature and Pressures

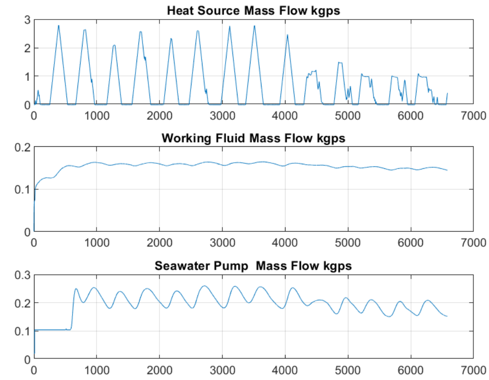

(b) Mass flow rates

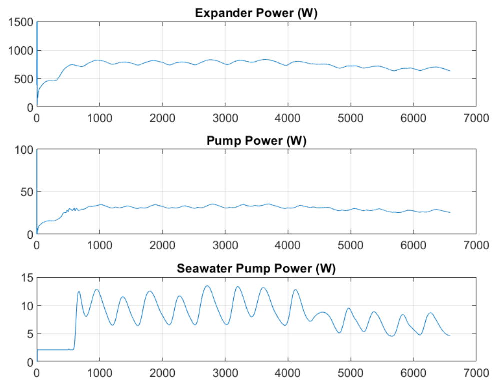

(c) Powers

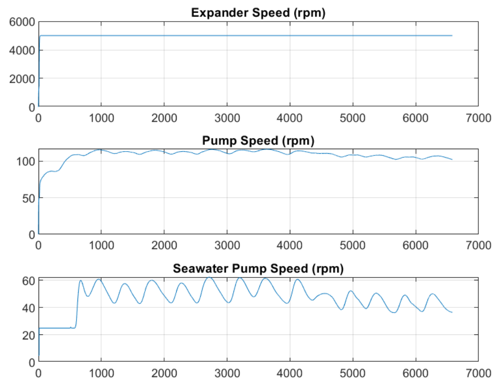

(d) Speeds

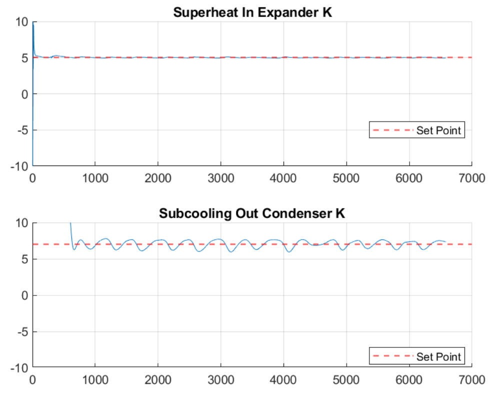

(e) Superheating and subcooling

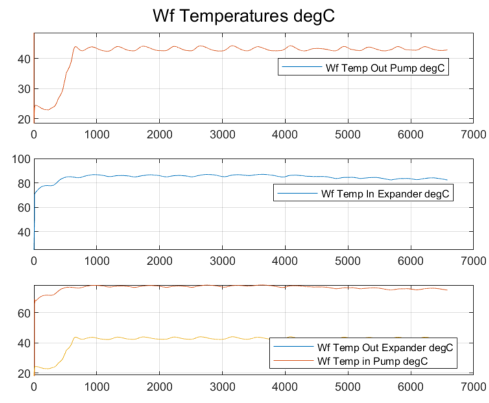

(f) Working fluid temperature

Figure 25: Dynamic simulation results for Novec649 model with Volumetric Expander.

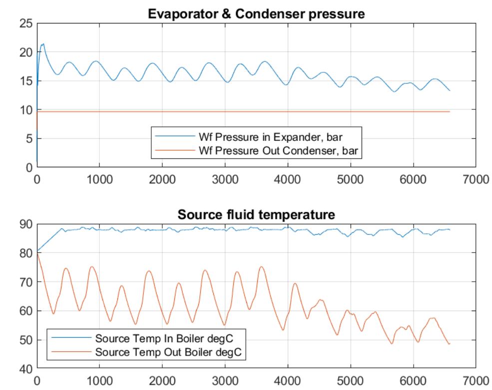

(a) Source temperature and Pressures

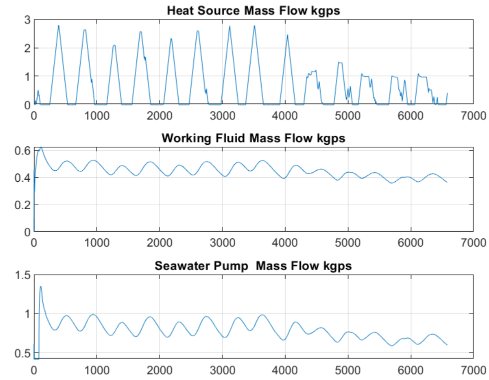

(b) Mass flow rates

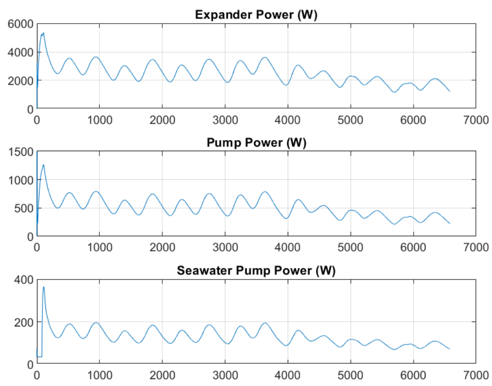

(c) Powers

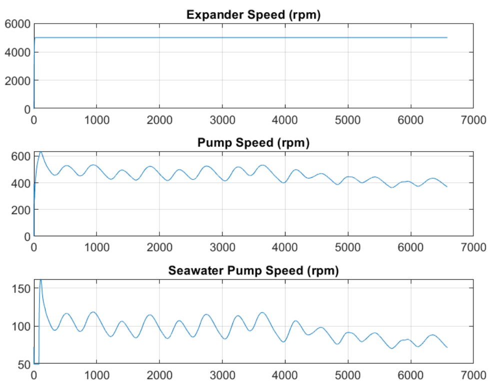

(d) Speeds

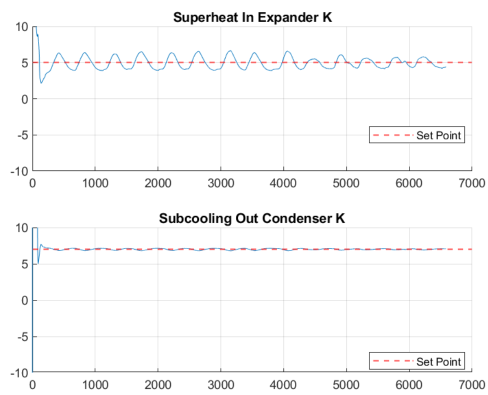

(e) Superheating and subcooling

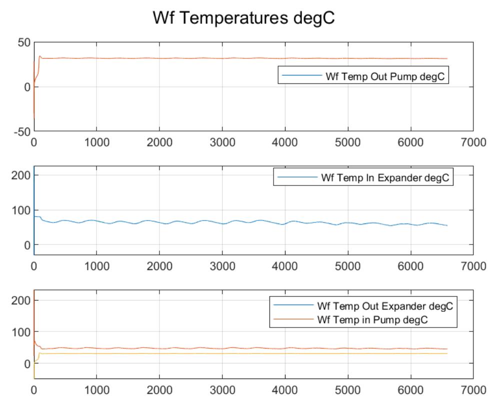

(f) Working fluid temperature

Figure 26: Dynamic simulation results for R1234yf model with Volumetric Expander.

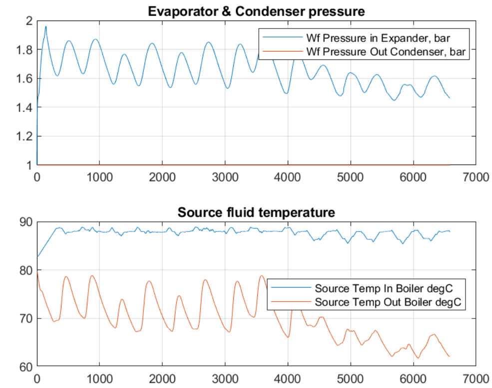

(a) Source temperature and Pressures

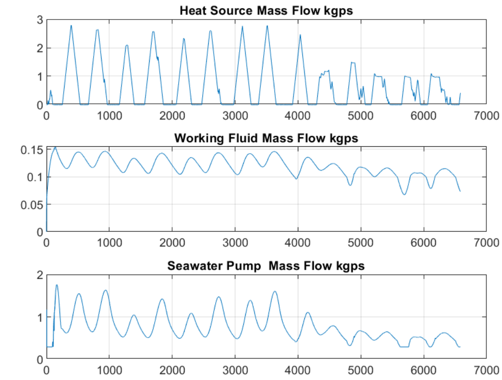

(b) Mass flow rates

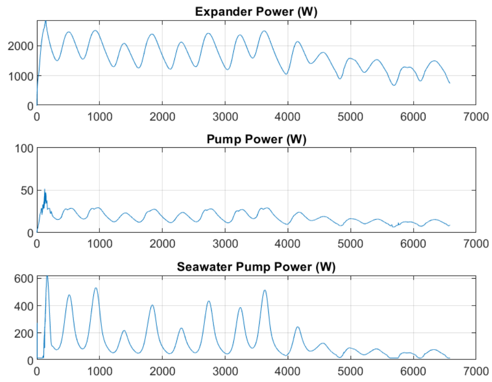

(c) Powers

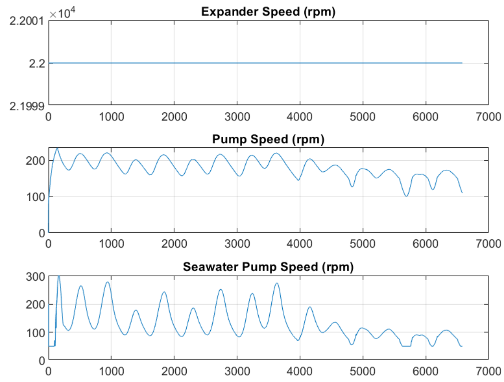

(d) Speeds

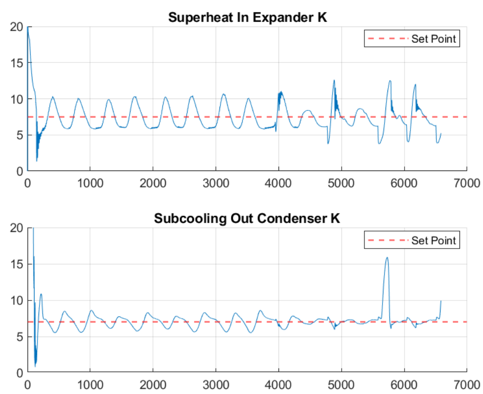

(e) Superheating and subcooling

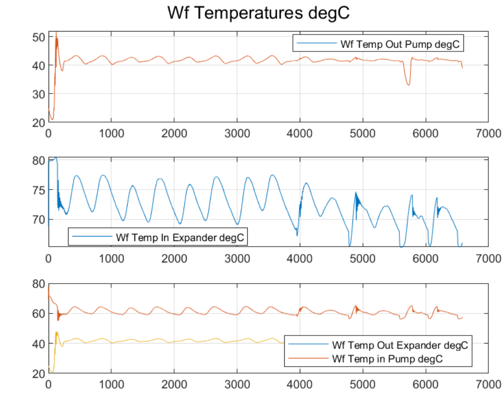

(f) Working fluid temperature

Figure 27: Dynamic simulation results for Cyclopentane model with Turbine Expander.

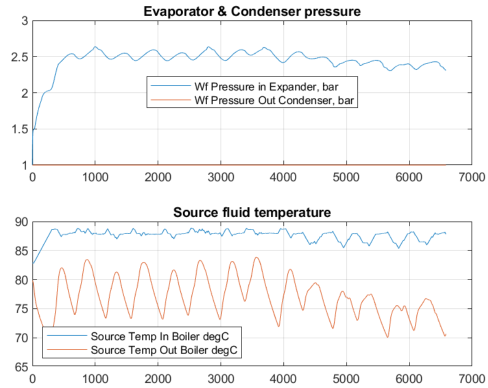

(a) Source temperature and Pressures

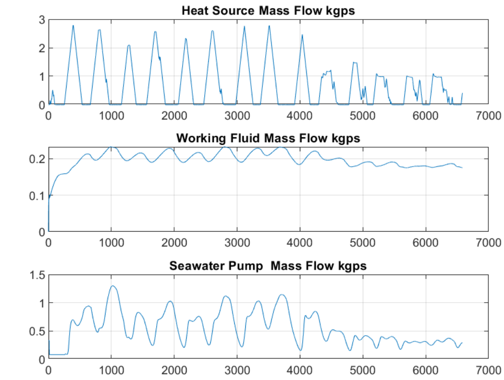

(b) Mass flow rates

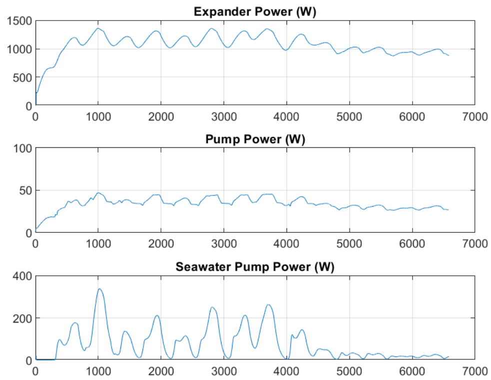

(c) Powers

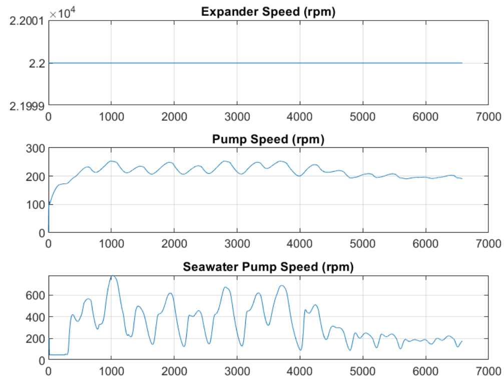

(d) Speeds

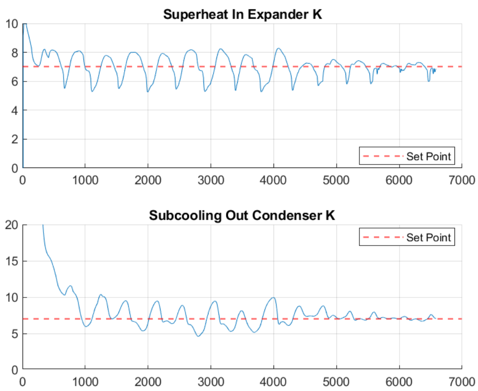

(e) Superheating and subcooling

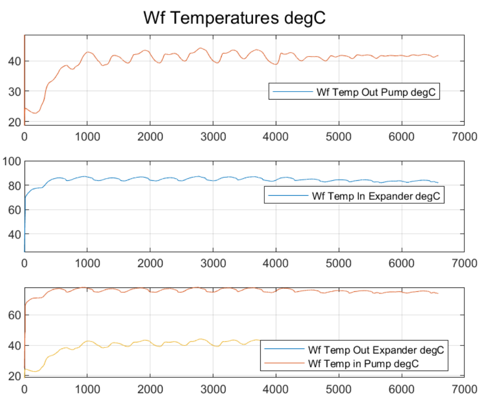

(f) Working fluid temperature

Figure 28: Dynamic simulation results for Novec649 model with Turbine Expander.

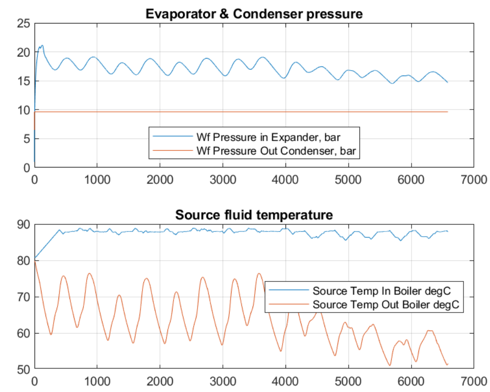

(a) Source temperature and Pressures

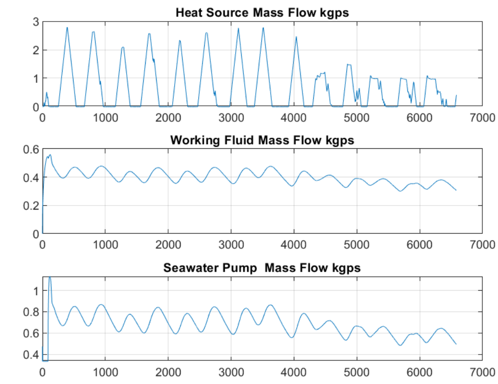

(b) Mass flow rates

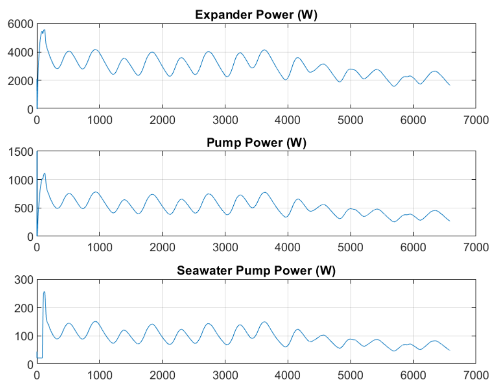

(c) Powers

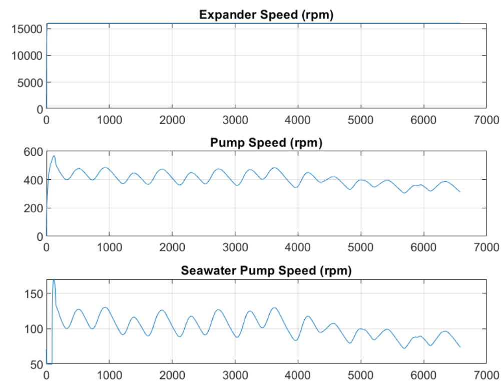

(d) Speeds

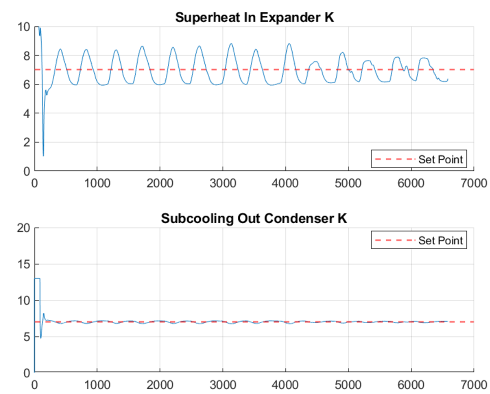

(e) Superheating and subcooling

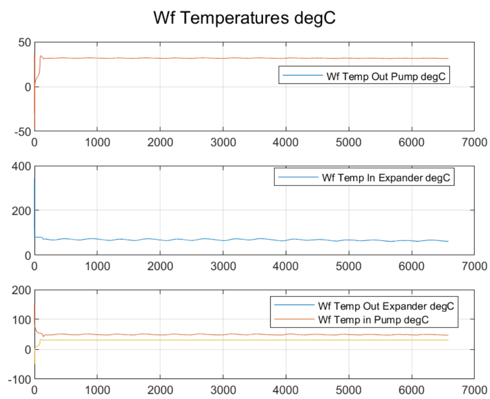

(f) Working fluid temperature

Figure 29: Dynamic simulation results for R1234yf model with Turbine Expander.

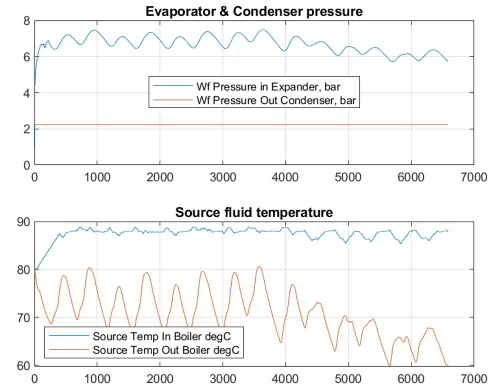

(a) Source temperature and Pressures

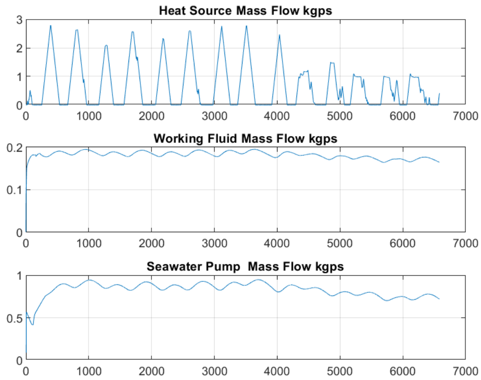

(b) Mass flow rates

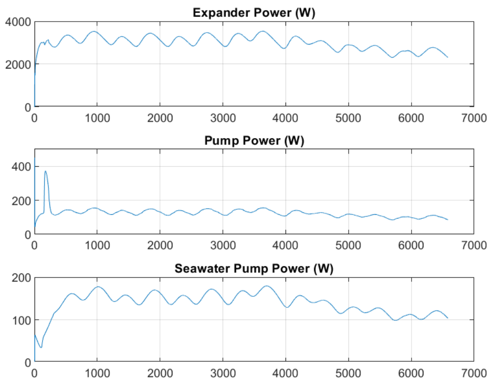

(c) Powers

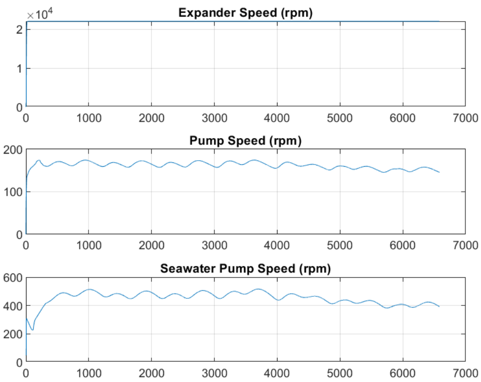

(d) Speeds

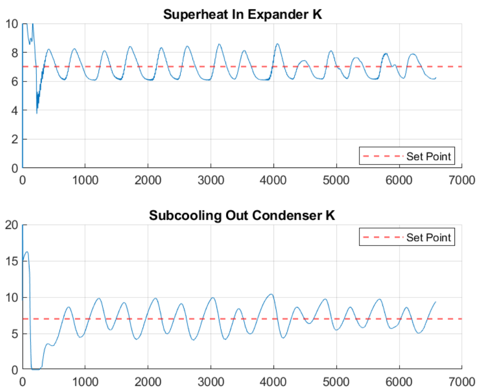

(e) Superheating and subcooling

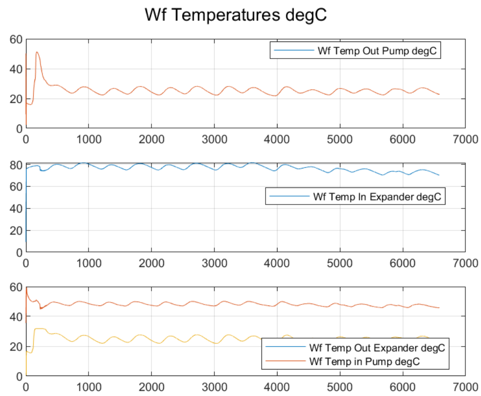

(f) Working fluid temperature

Figure 30: Dynamic simulation results for R1234ZE model with Turbine Expander.